UNIVERSITY OF VERONA

DEPARTMENT OF NEUROLOGICAL,
NEUROPSYCHOLOGICAL, MORPHOLOGICAL
AND MOVEMENT SCIENCES

GRADUATE SCHOOL
OF SCIENCES ENGINEERING MEDICINE

PHD PROGRAM IN NEUROSCIENCE

XXII CYCLE

BEHAVIOUR OF ENDO-LYSOSOMAL AND MITOCHONDRIAL COMPARTMENTS IN HUMAN NCL FIBROBLASTS *IN VITRO*

S.S.D. MED/26

Coordinator: Prof. Leonardo Chelazzi

Tutor: Prof. Alessandro Simonati

Student: Dr. Francesco Pezzini

INDEX

1. ABSTRACT

Neuronal ceroid lipofuscinoses (NCL) are degenerative disorders of childhood, which affect the central nervous system (CNS). NCL belong to the wider group of lysosomal storage diseases and they are characterized by the accumulation of endo-lysosomal material with specific ultrastructural features, both in neuronal cells and other peripheral tissues. NCL arise from either primary or secondary involvement of the lysosomal compartment, since mutated NCL proteins reside not only in the lysosomes but also in other cellular structures, such as the endoplasmic reticulum.

Over last 30 year ten NCL forms have been identified according to clinical, pathological and molecular criteria; moreover, eight NCL genes have been cloned, coding for proteins of specific and different functions. Therefore, today, NCL represents the acronym of a group of genetically different disorders of the CNS, leading to progressive shrinkage of the brain.

The main issue in the NCL pathology is the comprehension of which cellular mechanisms are involved in neuronal cell death in these conditions. Recently the attention has been addressed mainly to the pathogenetic role that the abnormal storage may exert on the cellular homeostasis and survival, even through apoptotic cell death. Moreover, a role for autophagy is also under scrutiny, since morphological and molecular evidences suggest the activation of this cellular mechanism both in humans and animal models of disease.

The aim of this doctorate project was to analyze *in vitro* the cellular behaviour of human genetically determined NCL fibroblasts derived from skin biopsies of patients affected with NCL forms, harbouring mutations on CLN1, CLN3, CLN5, CLN6 and CLN7 genes. Specifically, fibroblasts cell lines were analyzed in a 'prolonged culture paradigm' in order to assess which cellular responses could be activated by NCL cells, carrying a pre-existing endo-lysosomal dysfunction, to cope with the aging process *in vitro*.

We focused our attention principally on the evolution of the endo-lysosomal system during the prolonged growth; at the same time, we checked the mitochondria functionality and the activation of the apoptotic pathway. Both morphological and biochemical tools were used.

The morphological investigation of the endo-lysosomal system revealed that the aging of NCL cultures was associated with a progressive accumulation of lysosomal elements (lysosomal bodies, autolysosomes and empty vacuoles) in different manner as compared to controls. Furthermore, a different behaviour in the accumulation process of dense bodies and single membrane vacuoles was seen between CLN1 and the other forms. The detection

of autophagosomes led to investigate the autophagic pathway, that was found to be activated in several cell lines, regardless the NCL forms and the severity of mutation. Moreover, the morphological alterations of the endo-lysosomal compartment occurring in all NCL cell lines affected the mitochondrial network and the distribution of polarized mitochondria as well. No evidences of apoptotic activation were seen under basal conditions during the prolonged growth in all the cell lines analyzed. However, the treatment with the apoptotic chemical inducer Staurosporine revealed a different activation of the caspase-3 dependent apoptosis in two CLN1 lines as compared to the other NCL forms and controls. These results suggested that autophagy is activated in NCL fibroblasts, probably as a rescue cellular program to cope with the endo-lysosomal stress, intensified by the prolonged growth *in vitro*. At the same time, mitochondria, a vital compartment for the cell survival, were secondary affected in this *in vitro* model, whereas the indirect evidence of involved apoptotic pathway in CLN1 only seems to be consistent with recent scientific reports.

2. ACKNOWLEDGEMENTS

I would like to thank sincerely professor Alessandro Simonati to give me the opportunity to study and complete this doctorate project and to help me during these years with great, continuous and enthusiastic support as well.

Moreover, I would like to thank the Neuropathology Laboratory, all the guys and the staff, in particular Dr. Paola Tonin and Maria Marconi for the mitochondrial respiratory chain investigation and Floriana Gismondi for the electron microscopy analysis.

Finally, a very special thank to my *Family*.

3. INTRODUCTION

LYSOSOMES AND LYSOSOMAL STORAGE DISEASES (LSD)

Lysosomes and the endo-lysosomal system

The endo-lysosomal compartment of the cell include different membrane organelles that interact together through specific targeting mechanisms and fusion processes in order to degrade, sort and recycle material of different origin (Vellodi, 2005; Sleat et al, 2007; Lubke et al, 2009). The endo-lysosomal system is made up principally of *early endosomes*, localized prevalently to the cell periphery, *late endosomes*, that are perinuclear and *lysosomes*. Lysosomes are ubiquitous, small, single membrane organelles marked by a low lumen pH that contain many hydrolytic enzymes. These enzymes are responsible for the capability to degrade the substrates that are carried to lysosomes throughout different cellular pathways. Moreover, the lysosomal membrane is composed by many structural proteins that accomplish different tasks, such as maintenance of low pH within lysosomes (as in the case of proton pump V-type H+ ATPase), fusion process and transport and recycling of cellular component between cytosol and lysosomal lumen. However, the precise functions of most part of lysosomal membrane proteins remain still unclear (Saftig and Klumperman, 2009).

Lysosomal enzymes that have to be delivered to lysosomes follow specific routes among different cellular compartment. They are synthesized as inactive precursors in the rough endoplasmic reticulum (ER), modified by N-glycosylation in the lumen and then sorted by vesicles budding from ER to the Golgi apparatus. Once here, the precursors are again post-translationally modified. An important modification in the Golgi apparatus is the acquisition of mannose 6 phosphate (M6P) residue that is recognized by a specific receptor (M6Pr), allowing to sort proteins destined to lysosomes from those that have to be secreted. However, several proteins are correctly targeted to lysosomes without M6Pr pathway, probably throughout other less-known routes. Moreover, a portion of newly synthesized enzymes is not directly captured by M6P-receptor in the Golgi but they are secreted out of the cell and subsequently endocyted from neighbouring cells via M6Pr, localized on the plasma membrane. Finally, lysosomes are the last stage of maturation of lysosomal enzymes, where they become functionally active. Despite knowledge about the maturation pathway of hydrolytic enzymes, less it is known about the sorting and targeting mechanisms of lysosomal membrane protein.

Lysosomes and the degrading pathways of the cell: role in autophagy

Lysosomes play an essential role in the degradative pathways of the cells (Walkley, 2009). They receive different substrates both from outside (through endocytosis or phagocytosis according to the size of the material) and inside the cell (through the autophagic pathway).

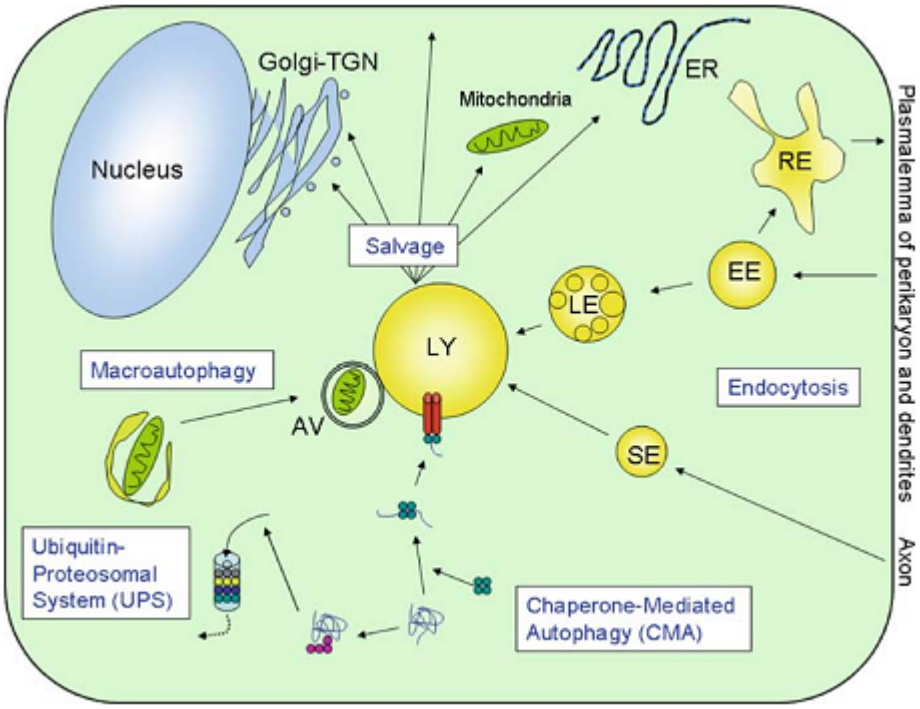

Figure 1.
Central role of lysosomes in the degrading pathway, represented for neuronal cells. Lysosomes receive cargos from different elements of endo-lysosomal system, such as autophagic vacuoles and endosomes. Moreover, lysosomes interact with two other degradative pathways, UPS and CMA. Lysosomes are not simply a deadly point: many components arriving in the lysosomes can be delivered to other cellular compartment through 'salvage' pathways. EE, early endosomes; LE, late endosomes; LY, lysosome; AV, autophagic vacuole; SE, signalling endosome; RE, recycling endosome; ER, endoplasmic reticulum (from Walkley, 2009).

As regards the degradation of cellular elements, the two main degradative pathways of the cells are macroautophagy, also referred to autophagy, and ubiquitin-proteosome system (UPS; Winslow et al, 2008). UPS, through the bind of ubiquitin residues to the target protein, is responsible for the degradation and recycling of short-lived cytosolic and nuclear proteins. The ubiquitin-tagged proteins are carried to a 2000 kDa multi subunit complex, the proteasome, and proteolitically cleaved inside this 'barrel-shape' complex. Due to the specificity of the process and the small size of the proteasome, many proteins are unable to be degraded by the UPS, including oligomers and proteins in organelles. On the other side, autophagy is the main mechanism by which cells remove and at last degrade

bulk cytoplasmic components (Levine and Kroemer, 2008; Mizushima et al, 2008 and 2010). Autophagy contributes to maintain cellular homeostasis and carries out many important functions in physiological processes of the cell, such as generation of ATP and nutrients in starved conditions, clearance of cellular debris and damaged organelles and finally elimination of unfolded proteins, in association with the unfolding protein response (UPR) system in the so called 'chaperone mediated autophagy' (CMA). Lysosomes are key elements of the autophagic pathway, because the autophagic cargo could be degraded only after the fusion with lysosomes. However, lysosomes could be not simply consider as the final step of the degrading pathway of the cell, because they are able to recycle cellular components and to secret their content after fusion with the plasma membrane.

The early step of the autophagic process is characterized by the formation of double-membrane structures, called autophagosomes, that surround cytoplasmic components of the cell, including organelles such as mitochondria. In the middle and late steps, autophagosomes fuse with lysosomes to form autophagolysosomes (called also autolysosomes), in which lumen components are degraded by lysosomal hydrolases. The different phases of the autophagic process rely on the functions of autophagic related proteins (Atg), in particular the Atg12-Atg5 complex and Atg8/LC3 (microtubule associated protein 1 light chain 3). Atg12-Atg5 is an ubiquitin-like enzymatic complex that convert LC3 from a cytoplasmic isoform I to an autophagosome-associated isoform II, that is inserted in the double membrane during the autophagosomal formation (Genge and Klionsky, 2008). In particular, this complex add a phosphatidylethanolamine (PE) residue to the LC3 I, that increases the hydrophobicity of isoform LC3 II and generates different mobility patterns on SDS-page electrophoresis, allowing to distinguish the two isoforms by western blot analysis. Thus, the conversion of LC3 between isoform I to isoform II is marked by the identification of two distinct bands, at 16 kDa and 14 kDa, corresponding to LC3 I and LC3 II respectively. Subsequently, mature autophagosomes fuses with lysosomes forming the autophagolysosomes. After the fusion, the release and subsequent activation of hydrolytic enzymes in the lumen bring on the degradation of the inner membrane, leaving single membrane autophagic vacuoles with partially degraded material inside. So, LC3 II is partially removed from the autophagolysosomal membrane and returns finally to the cytosol. For these reasons, the use of electron microscopy analysis allows to detect both autophagosomes and later autophagic vacuoles, whereas LC3 II marked mainly the autophagosomes and therefore an early step of the autophagic pathway (Tadsemir et al, 2008; Eskelinen, 2008). Increased level of autophagosomes formation

could reflect an enhancement or a block of the autophagic pathway and this condition is thought to be related to a type of cell death (so called 'autophagic cell death Type II'; Maiuri et al, 2007). However, it is more correct to say that autophagic cell death happens '*with* autophagy' than '*through* autophagy' because autophagy seems to act as a rescue program in order to prolong cell survival and prevent cell death in response to different toxic stimuli (as in the cases of protein aggregates in Huntington and Alzheimer diseases). Thus, in spite of its function in maintaining cellular homeostasis, an over-activation of the autophagic process could be detrimental for the cell survival.

Lysosomal storage diseases

The complexity of lysosome biogenesis and the large amount of lysosomal functions, briefly described above, imply that many alterations, occurring at different steps of these processes, could severely affect the homeostasis of lysosomes. Lysosomal storage diseases (LSD) are rare genetic metabolic disorders caused by alterations on proteins generally involved in lysosomal functions, leading to storage of undigested cellular material (Walkley, 2009). With only few exceptions, LSD are recessively inherited disorders and to date more than 50 different forms are known. Despite the fatal outcome, LSD patients are normal at birth and start showing clinical symptoms after several weeks in the most severe cases or commonly after a few years. Different organs are the main targets of LSD, such as bones, bone marrow, skeletal muscle, liver; the central nervous system (CNS) is affected in about two-third of LSD. Yet it is noteworthy that the systemic manifestations depend mainly on the distribution of the substrates in the different tissues. With regard to CNS, many LSD show a chronic degeneration of cortical and cerebellar neurons associated with an intense glial response.

Originally, LSD were divided on the basis of the biochemical substrates that accumulate in the cell as a consequence of the lysosomal alteration. Nevertheless, the distinction on the basis of stored material is quite ambiguous, because different LSD could share the same storage materials or a mixture of them. More precise is the classification on the basis of the biological process altered in a specific condition, independently from the stored material. Thus, LSD could arise from deficiency in enzymatic or non enzymatic proteins, localized either in lysosomes or in other cellular compartments. For this reason, we could identify 'primary' lysosomal disorders, in which the altered protein is a lysosomal constituent and 'secondary' lysosomal disorders. In the former case, the molecular defect can affect either hydrolytic enzymes of lysosomes (as well as their ancillary activating protein) or structural

proteins of lysosomal membrane. In the latter, alteration of lysosomes function may originate from mutations on proteins that reside in other cellular compartments. Indeed, several LSD occur due to alterations in ER or Golgi resident enzymatic or structural proteins that could affect the synthesis, post-translational modifications, sorting or stability of different lysosomal proteins. For instance, mucopolysaccaridosis II and III rise from alterations in Golgi enzymes responsible for the M6P modification. This leads to a global defects on lysosome biogenesis because many new synthesized lysosomal hydrolytic proteins fail to be targeted to lysosomes in an appropriate manner. Another example is the multiple sulfatase deficiency (MSD) that affects the entire sulfatase family, at least seven members of which are lysosomal enzymes, specifically involved in the degradation of sulfated glycosaminoglycans, sulfolipids or other sulfated molecules. Neuronal Ceroid Lipofuscinoses (NCL) represent a fascinating group of LSD that share common clinical features in spite of biological heterogeneity as regards the localization and function of the proteins involved. For this reason, NCL represent a good model to investigate the lysosomal function and the biological alteration generating from different cellular compartments that lead to functional lysosomal unbalance.

NEURONAL CEROID LIPOFUSCINOSES

Neuronal ceroid lipofuscinoses (NCL) are a group of degenerative disorders of childhood mainly affecting CNS, and are characterized by the storage of lysosomal material with specific ultrastructural features, both in neuronal cells and other peripheral tissues (Jalanko and Braulke, 2009; Simonati et al, 2009). NCL are genetically determined and inherited as recessive autosomic traits (Mole et al, 2005). NCL exhibit a worldwide estimated frequency of 1 affected person per 12.500 live newborns; in Italy a recent survey of genetically determined cases over a 15 year period resulted in an incidence of 0.90/100.000 births (unpublished observations).

Historical notes

The first description of a NCL has been commonly attributed to a Norwegian physician, Dr Otto Christian Stengel (Zeman et al, 1970). In 1826 he described four siblings that at the age of 6 began to develop blindness, progressive motor deterioration and loss of speech, epileptic seizures and premature death. This case report, written in Norwegian, remained unnoticed for a century, until other patients with visual and motor impairment

were studied by several clinicians (Tay Sachs, Batten, Vogt, Spielmeyer, Jansky and Bielschowsky). On the basis of similar clinical features and evidences of accumulation of lipidic material in nerve cells, these disorders were classified as 'amaurotic family idiocies'. Only in the early 1960' biochemical and ultrastructural studies on the storage material revealed the heterogeneous nature of this group of disorders, allowing to separate the conditions that store gangliosides from those that store lipopigment such as lipofuscin. In order to distinguish the latter group from gangliosidosies or Tay Sachs disease, Zeman and Dyken proposed the new term of 'neuronal ceroid lipofuscinoses' (Zeman and Dyken, 1969).

Clinical features and pathological findings

NCL are a heterogeneous group of disorders that share common clinical symptoms and histopathological features. NCL occur mainly in childhood and are marked by retinopathy leading to visual impairment, gait abnormalities (due to the cerbellar involvement and spasticity), epileptic seizures associated with psychomotor decline and dementia. Most severe forms have a fatal outcome within the second decade of life.

From a histopathological point of view, NCL are characterized by a severe cerebral and cerebellar atrophy due to widespread neuronal cell loss. Affected neurons at biopsy show storage of autofluorescent, PAS and Sudan B black positive glicolipidic inclusions that present characteristic ultrastructural features (granular osmiophilic deposits, GRODS; curvilinear bodies, CB; rectilinear profile, RP; fingerprint profile, FPP). This peculiar storage material is also termed cytosomes. Even if the most affected target in NCL is the CNS, cytosomes could be detected in other peripheral tissues, such as skin, muscle, gut and peripheral blood cells without evidence of dysfunction of such tissues. By the end of '80s biochemical studies on a sheep NCL model and human biopsies revealed that cytosomes were largely composed of protein despite of lipid. In particular, the majority of NCL forms contain mainly subunit c of ATP synthase (SCMAS), whereas in the infantile form the most abundant stored components are sphingolipid activator protein (saposins, SAP) A and D.

NCL classification

Historically, NCL were divided in four distinct NCL forms on the basis of the age of onset of the early symptoms: Infantile (INCL), Late-Infantile (LINCL), Juvenile (JNCL)

and Adult (ANCL) forms. A rare congenital NCL form has also been described (Siintola et al, 2006; Steinfield et al, 2006).

Classically, the diagnosis of NCL is based on both the description of clinical symptoms and the identification of cytosomes in rectal and skin biopsies or on lymphocyte pellet. However, in the '90s advances in genetic analysis allowed the discovery of gene causing classical infantile form CLN1 (Vesa et al, 1995) and juvenile form CLN3 (The International Batten Disease Consortium, 1995). Then, over the last decade, other NCL genes carrying many mutations were identified, expanding the spectrum of NCL genes and providing further elements for a more precise definition of this group of disorders.

To date, eight NCL genes and approximately 200 mutations have been identified (comprehensively reported and listed in the NCL Mutation Database**,** http://www.ucl.ac.uk/ncl/). The recent classification is based prevalently on genetic knowledge and clinical criteria and distinguish among ten different NCL forms, from to CLN1 to CLN10 (table 1). Five different genes (CLN2, CLN5, CLN6, CLN7 and CLN8) are responsible for the Late Infantile NCL form and its variants, but it is important to note that different mutations in a single gene may result in different phenotypes, including different ages of onset. CLN4 and CLN9 genes have not been cloned so far. In addition, several NCL cases fail to show mutations in any of known NCL genes, so new NCL genes related to these 'orphan' forms have to be discovered yet. Orthologous NCL gene were also described on several animal models, such as sheep, dogs and mouse. These animal models mimic various NCL clinical and histopathological features, such as motor decline, reduced lifespan, lipofuscin inclusion and extended neuronal cell death (Jalanko and Braulke, 2009). Moreover, other models such as yeast cells, *caenorhabditis elegans*, *drosophila melanogaster* and zebrafish were genetically modified in NCL related genes and extensively employed in order to unravel NCL protein functions and the alterations associated with these mutated proteins (Cooper et al, 2006; Haines et al, 2009).

NCL diagnosis

Diagnosis of these disorders is now performed by description of clinical symptoms and mutational confirmation. Detection of cytosomes, an essential method in the 'pre-genetic era', is still very useful in the diagnosis because it could address to the appropriate genetic analysis for the determination of the precise NCL form. Moreover, biochemical enzymatic tests are also available for three NCL forms, specifically CLN1, CLN2 and CLN10, which

are caused by alterations in three specific hydrolytic lysosomal enzymes (Kohlschütter and Schulz, 2009).

NCL gene products

The characterization of NCL genes confirms that NCL are an heterogeneous group of disorders, despite similar clinical phenotypes. Specifically, NCL genes code for proteins that are localized in the lysosomes, or in other cellular compartments, such as the endoplasmic reticulum (ER), the Golgi apparatus and the synaptic vesicles. For this reason, it has been proposed to divide NCL as '*primary'* and '*secondary'* lysosomal disorders (table 1). Specifically, three forms (CLN1, CLN2 and CLN10) could be considered as 'primary' lysosomal disorders because the affected proteins are hydrolytic lysosomal

	NCL Form	Protein	Protein topology & function	Cellular localization	Cytosomes & storage material
Primary lysosomal NCL	**CLN1** Infantile vLate Infantile vJuvenile Adult	PPT1 (Palmitoyl Protein thioesterase);	Soluble enzyme: - removal of palmitate by hydrolisis of thiosteric bound in S-acylated protein	Lysosome; Synaptic vesicles; Synaptosomes; Axons	GROD / SAP A and D
	CLN2 cLate Infantile	TPP1 (Tripeptidyl Peptidase I);	Soluble enzyme: - removal of tri-peptides	Lysosome;	CVB (RP, FPP) / SCMAS
	CLN10 Congenital vJuvenile	Cathepsin D;	Soluble enzyme: - hydrolisis of shingolipid, pro-saposins	Lysosome;	GROD / SAP A and D
Secondary lysosomal NCL	**CLN3** Juvenile	CLN3 protein;	Membrane protein: - arginine transport? - maintainance of pH? - vesicular trafficking?	Lysosomes-Endosomes; Golgi apparatous; Synaptosomes;	FPP (RP, CVB) / SCMAS
	CLN4 Adult	?	?	?	GROD-like / SCMAS
	CLN5 vLate Infantile	CLN5 protein;	Membrane/soluble protein: - unknown function	Lysosome; Axons;	FPP, CVB, RP / SCMAS
	CLN6 vLate Infantile	CLN6 protein;	Membrane protein; - unknown function - dimerization ?	Endoplasmic reticulum;	CVB, FPP, RP / SCMAS
	CLN7 vLate Infantile	MSFD8/CLN7 protein;	Membrane protein: - transporter	Lysosome;	FPP (RP, CVB) / SCMAS
	CLN8 vLate Infantile Northen epilepsy	CLN8 protein;	Membrane protein: - lipid sensor?	Endoplasmic reticulum;	CVB, GROD / SCMAS
	CLN9 vJuvenile	CLN9 protein;	Regulatory enzyme;	?	CVB, GROD / SCMAS

Abbreviations:

c: classical; v: variant; GROD: granular osmiophilic deposits; CVB: curvilinear bodies; FPP: fingerprint profiles; RP: rectilinear profile; SAP A and D: saposins A and D; SCMAS: subunit c of mitochondrial ATP synthase

Table 1.
NCL classification and related gene product.

enzymes (palmitoyl protein thioesterase PPT-1, tri-peptidyl peptidase TPP-1 and cathepsin D respectively). Otherwise, the other forms could be defined 'secondary' lysosomal disorders since the altered proteins are localized on different membranous cellular compartments (including the lysosomal membrane) and their functions are not fully determined yet. The comprehension of the functions of the single NCL proteins and the molecular cross-talk among them in a putative common metabolic pathway are the major challenging issues in the NCL field.

CLN1

CLN1 gene resides on chromosomes 1p32 and encodes for palmitoyl protein thioesterase 1 (PPT1), an hydrolytic enzyme that catalyze the hydrolysis of thioesteric bond in S-acylated proteins and removes palmitate from them (Vesa et al, 1995). The substrates of PPT1 are not well-characterized so far; it has been shown that PPT1 removes palmitate residues from H-RAS, at least in vitro (Camp et al, 1993). PPT1 polypeptide is constituted by 306 amino acids, with 25 amino acid N terminal signal sequence that is cotranslationally cleaved. It contains three different N-glycosylation sites, necessary for its stability, and migrates with an apparent 35/37 kDa molecular weight. The crystal structure of bovine PPT1, that shows 95% of homology with human PPT1, has been characterized and reveal an α-β serine hydrolase structure, typical of lipases, in according to the palmitate removing function previously hypothesized (Bellizzi et al, 2000). Protein palmitoylation or, more specifically, S-acylation is a reversible post-translational lipid modification, which is of relevant importance in neurons, particularly in synaptic vesicle turnover (Prescott et al, 2009). PPT1 shows different features in neuronal and non neuronal cells. Several studies show that PPT1 is localized in lysosomes, but in brain tissue and cultured neurons it has also been detected in the cell soma, axonal varicosities and pre-synaptic terminals, including synaptosomes and synaptic vesicles (Verkruyse et al, 1996; Heinonen et al, 2000; Lehtovirta et al, 2001; Ahtiainen et al, 2003). Moreover, it has been demonstrated that PPT1 could homodimerize or oligomerize *in vivo* and that other cellular sorting pathways, in addition to the classical M6Pr route, could traffic CLN1p within neurons (Lyly et al, 2007). The precise function of PPT1 remains unclear but the lipase-like structure and the de-palmitoylation capability suggest that in neurons PPT1 acts near the cell membrane and it is involved in different important processes, such as endocytosis, vesicular trafficking, receptors recycling and targeting, synaptic function (Goswani et al, 2005). In particular, palmitoylation is a post-translational modification that is characterized

by the addiction of a carbon 16 saturated fatty acid in a reversible manner (Husseini and Bredt, 2002; Huang et al, 2005). This modification increases the protein hydrofobicity, facilitates membrane interaction with lipid bilayers and finally influences the cell sorting and trafficking of the modified protein. This process is very important for neuronal cell, because it may be involved in the correct cell sorting, axonal development, ion-channel clustering and synaptic function (Husseini and Bredt, 2002). In addition to the important functions on recycling of proteins in neurons, PPT1 seems to be related to the apoptotic cell death. As a matter of fact, an over-expression protects from apoptosis (Cho and Dawson, 2000) whereas a decreased expression enhances susceptibility to induced apoptosis in neuroblastoma cell line (Cho et al, 2000). Moreover, also TNF -induced apoptosis has been reported to be functionally altered in PPT1 deficient cell lines (Tardy et al, 2009).

Mutations in *CLN1* gene cause CLN1 disease and 45 different mutations have been described so far. The age of onset is typically around the first year of life for the classical infantile form, but some mutations are associated with other NCL forms, spanning from the late infantile to the juvenile forms (Simonati et al, 2009). Few adult cases are also been described (van Diggelen et al, 2001). The genetic mutational analysis of *CLN1* gene is often associated with a reliable enzymatic test on blood sample to determine the PPT1 activity. In same cases it is possible to correlate the clinical severity of disease with the residual enzymatic activity: mutations causing truncated protein or minimal residual activity tend to result in earlier onset and more rapid progression whereas milder mutations, such as missense mutations, result in later clinical onset and slower rate of neurodegeneration. The ultrastructural hallmark for all the CLN1 phenotypes form is the detection of GRODs in neuronal and peripheral tissue, including skin and rectal biopsies. The most abundant stored material are sphingolipid activator protein A and D (Ahtiainen et al, 2006). Which is the precise metabolic pathway leading to the origin of the glycolipidic and protein deposits remains still unknown.

CLN2

The *CLN2* gene is localized on chromosome 11p15 and encodes for the tripeptidyl peptidase 1 (TTP1), a lysosomal hydrolytic enzyme broadly expressed in different tissues (Sleat et al, 1997). CLN2 protein is synthesized as an inactive precursor of 563 amino acids, with a 19 amino acids signal peptide co-translationally cleaved in the ER lumen, and then processed to mature form in the lysosome (Golabek et al, 2003). It contains 5 distinct

glycosylation sites necessary for the maturation and appropriate targeting of the protein (Wuiek et al, 2004). TPP1 is an hydrolytic enzymes that is able to remove tripeptides from proteins. The crystal structure has been recently characterized, allowing to unravel the catalytic site and the conformational changes during the maturation of the protein (Pal et al, 2009; Guhaniyogi et al, 2009; Walus et al, 2005). *In vivo* substrates of TPP1 are still unknown, but *in vitro* studies showed that subunit c of mitochondrial ATP synthase is processed by TPP1 (Ezaki et al, 1999). Interestingly, SCMAS, a highly hydrophobic subunit of ATP synthase, is the mainly protein material included in cytosome typical of CLN2 and other NCL forms. Other putative *in vitro* targets are beta amyloid peptide, angiotensins I and II, glucagons, cholecystokinin and neuromedin but no one of these substrates are detected in the storage material.

Mutations in *CLN2* gene lead to classical late infantile NCL and to date more than 50 mutations have been described. All the mutations lead to a reduction of enzymatic activity and result in a clinical phenotype that show common clinical features. CLN2 patients show the first symptoms classically in late infancy (between 2 and 5 years); seizures and ataxia are the clinical hallmark, followed by progressive mental and motor decline. Visual impairment begins later and death occurs in the second decade. Ultrastuctural analysis of the cytosomes reveals the presence of curvilinear bodies that are the hallmark of CLN2 disease; in addition, FPP are often detected. The 85% of the storage material is made up of SCMAS, but also SAP A and D are present in lower amount (Jalanko and Braulke, 2009; Palmer et al, 1992).

CLN3

The *CLN3* gene resides on chromosome 16p1, contains 15 exons spanning 15 kb and encodes for a 438 amino acids polypeptide. CLN3 protein is an integral membrane protein, which presents six transmembrane domain, with both N- and C-termini facing to the cytoplasm. As for other NCL proteins, the over-expression assay indicates that CLN3 localizes in lysosomes on non-neuronal cells, whereas on neuronal cell the protein has been detected in the endo-lysosomal compartment and in synaptosomes. Moreover, other various subcellular localizations have been described, including mitochondria, Golgi apparatus and late endosomes. Taking together, these finding suggest that CLN3p may shuttle across Golgi apparatus and plasma membrane through the endo-lysosomal pathway (Jalanko and Braulke, 2009).

The precise CLN3p function has not been characterized so far, but recent findings on yeast cells and mouse models shed lights on the processes in which CLN3 protein is involved. In particular, *Saccaromyces pombe* with a deletion in *CLN3* homologue gene (*btn-1Δ*) showed increased pH in vacuoles, which are the yeast organelle corresponding to lysosomes in mammalian cell (Gachet et al, 2005). Interestingly, it has been reported that lysosomal pH is affected in different NCL fibroblasts, including juvenile NCL fibroblasts, suggesting a role for CLN3/btn1-Δ protein in the maintenance of lysosomal pH (Holopainen et al, 2001). Moreover, other putative functions of CLN3p have been hypothesized, including lysosomal arginine transport, membrane fusion, vesicular trafficking, cytoskeletal linked function, autophagy, apoptosis and proteolipid modifications (Jalanko and Braulke, 2009; Rusyn et al, 2008).

Mutations in *CLN3* gene give rise to the juvenile form of NCL. JNCL represents the most common form of NCL world-wide. More than 40 different mutations have been identified so far. The most frequent mutation is a large deletion of a 1.02 kb that erase exons 7 and 8 in *CLN3*, producing a severe truncating protein. If this protein retain a residual activity is still debated. Other mutations usually lead to retention of the mutated protein in the ER compartment; however, some mutations, linked to a milder phenotype, seem to allow the mutated CLN3 protein to leave the ER (Järvelä et al, 1999; Haskell et al, 2000; Jalanko and Braulke, 2009). JNCL patients show the first symptoms between 5 and 10 year, in particular the visual impairment due to retinal degeneration is the first manifestation. Successively, JNCL patients develop mental deterioration, followed by epilepsy and motor decline. Death occurs in the third decade, or even later. Ultrastructural analysis reveals the presence of FPP, in association with CVB and RP in some cases, either within lysosomal bodies or surrounded by a single membrane vacuoles. Vacuoles are hallmark of CLN3 and have been detected both in neurons and peripheral tissues, such as in skin biopsies and lymphocytes. In particular, the detection of vacuolated lymphocytes, even on a blood smear, is a very useful tool in the diagnosis of CLN3 form, leading to the appropriate mutational analysis of the gene. The storage deposits contains mainly SCMAS.

CLN4

The CLN4 form, termed also Kufs disease, is an heterogeneous group of NCL with clinical manifestations in the adult age (ANCL). Two major ANCL phenotypes are known. The ultrastructural analysis of storage material and the cytosomes distribution are very important tools in the differential diagnosis with other progressive dementia of adulthood.

Actually, GROD-like deposits, in association with CVB and FPP, are often detected in neuronal cells and other tissues. However, in a few cases negative ultrastructural analysis of peripheral tissues makes a cerebral biopsy necessary to address to the appropriate diagnosis (Simonati et al, 2009). Interestingly, CLN4 is the only known NCL form in which an autosomic dominant trait of inheritance has been reported. At present it is not known how many putative genes might be responsible for this disease.

CLN5

CLN5 gene is localized on chromosome 13q21 and encodes for a 407 amino acid polypeptide with a predicted molecular weight of 46kDa (Savukoski et al, 1998). CLN5 mRNA contains four different initiation methionines sites and an *in vitro* translation assay demonstrated the production of 4 different polypeptides with apparent molecular weight raising from 37 to 47 kDa. CLN5 function and its topology are still unclear. Mouse CLN5 is reported to be a soluble protein (Holmberg et al, 2004); moreover, human CLN5 contains mannose-6-phosphate residues indicating the existence of soluble CLN5 variants (Isosomppi et al, 2002; Sleat et al, 2006; Schmiedt et al, 2010). The over-expression of *CLN5* indicated that CLN5p is localized in the lysosomal compartment, but in neurons, in the same way as CLN1p and CLN3p, it was detected also in the axons. Immunoprecipitation and in vitro binding assay suggests that CLN5p interacts with two other NCL protein, CLN2 and CLN3, suggesting for the first time the possible existence of a interaction among different NCL proteins (Vesa et al, 2002; Lyly et al, 2009). Recently, evidence has been provided of disease occurrence associated with CLN5p retention in the ER (Lebrun et al, 2009).

Alterations in *CLN5* cause a variant of Late Infantile NCL (Bessa et al, 2006; Cannelli et al, 2007; Savukoski et al, 1998). The first symptoms start classically between the age 2 and 6 years and are principally the mental decline followed by blindness, ataxia and epileptic crisis. The cytosomes that mark CLN5 form are CVB in association with FPP, but in same case also variant of rectilinear profile are observed. The major storage component is SCMAS.

CLN6

The *CLN6* gene lies on chromosome 15q22-23 and encodes for a 311 amino acid polypeptide formed by seven predicted transmembrane domains, with a cytosolic N-terminus and a lumen C-terminus. This protein resides on endoplasmic reticulum and in

neuronal cells is detected along neuronal extension in subdomains of a tubular ER network (Jalanko and Braulke, 2009). The function of CLN6 protein and the mechanism by which it could influence the accumulation of lysosomal material are unclear so far. In the same way as other NCL forms, CLN6 fibroblasts show increased lysosomal pH (Holopainen et al, 2001) and an altered degradation of endocytosed arylsulfatase A, probably due to an intracellular distribution of both M6Pr and endocytic adaptor proteins (Heine et al, 2004). However, neither sorting of newly synthesized cathepsin D, nor the activity of several lysosomal enzymes (CtsD, β-hexosaminidase and arylsulfatase A) were affected in CLN6 fibroblasts (Heine et al, 2004). Moreover, single membrane vacuoles have been detected on human biopsies, suggesting that the alteration of CLN6p could influence and trigger an autophagic response in vivo (Cannelli et al, 2009). It has been proposed that CLN6p is able to form dimers, so the effects of mutations could affect the correct localization or the capability of homodimerization.

Mutations in *CLN6* cause a variant late infantile NCL form. Clear-cut genotype-phenotype is not possible, because most of mutations show similar disease clinical course (Simonati et al, 2009). It could be speculated that milder phenotype depend on the residual capability of the CLN6 protein to dimerize. However, both intra and inter familial variability have been reported, supporting the idea of additional genetic or epigenetic determinants are important in NCL manifestations. Electron microscopy analysis on biopsies and cell show the accumulation of RP and FPP cytosomes, which contain prevalently subunit c of mitochondrial ATP synthase.

CLN7

The *CLN7* gene has been identified recently, in 2004, by genome-wide scanning and is located on chromosome 4q28.1-q.28.8. CLN7 encodes for a 518 amino acids polypeptide with 12 putative transmembrane domains. As suggested by the predicted molecular structure, CLN7 is a membrane protein and belongs to the large major facilitator superfamily (MSF) transporting specific classes of substrates, such as sugars, drugs, inorganic and organic cations and various metabolites (Siintola et al, 2007). The specific CLN7 substrate has not been characterized so far. Overexpression of protein indicates that CLN7 resides on the lysosomal membrane.

Mutations in *CLN7* gene result in a typical variant late infantile form, starting usually with epileptic seizures and cognitive decline. Progressive motor and mental decline associated with myoclonus and visual impairment lead to cell death in the early second

decade of life (Aiello et al, 2009). The storage material closely resembles the cytosomes of other vLINCL forms and made up of a mixture of FPP and RP, but CVB are also detected. Because of similar features within the heterogeneous group of vLINCL forms, the genetic investigation is necessary for a correct diagnosis, supporting the clinical and ultrastructural investigations.

CLN8

The *CLN8* gene lies on chromosome 8p23 and encodes a non-glycosylated 33kDa membrane protein of 286 amino acids. The CLN8 protein contains an ER-retrieval signal (the di-lysine motif KKRP) and it has been suggested that CLN8 protein shuttle between ER and ER-Golgi intermediate complex (ERGIC) (Lonka et al, 2000; Lonka et al, 2004). The precise structural conformation has not been characterized so far, but the CLN8 contains probably 5 transmembrane domains. The function is unknown, but using computational analysis, it has been shown that it belongs to the TRAM-Lag1p-CLN8 (TLC) molecular family proteins involving in biosynthesis, metabolism, transport and sensing of lipids (Winter et al, 2002; Riebeling et al, 2003). Mass spectrometry analysis of brain samples of EPMR patients demonstrated changes in the molecular composition of several phospho- and sphingolipid molecules which may lead to altered membrane properties and membrane proteins functions (Hermansson et al, 2005).

Mutations in *CLN8* cause childhood-onset NCL, which has remarkable phenotypic differences according to the underlying mutation. One Finnish phenotype, characterized by early juvenile onset and slowly progressive course, with epilepsy and cognitive deterioration (Progressive Epilepsy with Mental Retardation, EPMR), is associated with one homozygous missense mutation in the CLN8 gene (Ranta et al, 1999). Different mutations in *CLN8* (presumably leading to severe loss-of-function of the gene) were detected in patients from different ethnic backgrounds and affected with a more severe variant late infantile onset (vLINCL) phenotype with early onset myoclonus and visual failure, partially overlapping with classical late-infantile and juvenile forms of NCL (Ranta et al, 2004; Cannelli et al, 2006, Zelnik et al, 2007).

Ultrastructural analysis of CLN8 biopsies show a mixture of CVB, FPP and, less frequently, GROD-like storage in skin, muscle biopsies and lymphocyte, with SCMAS as the main stored material.

CLN9

CLN9 form is a variant LINCL form but the affected gene has not been characterized so far. Only four patients have been reported, resembling clinical symptoms similar to juvenile or CLN3 patients. Fibroblasts from these patients show several abnormalities: they are sensitive to apoptosis, they grow rapidly and manifest cell adhesion defect. Moreover, CLN9 protein could be involved in the regulation of dihydroceramide synthase, because fibroblasts show reduced levels of ceramide, dihydroceramide and sphingomyelin (Schultz et al, 2004; Schultz et al, 2006).

CLN10

The CLN10 *gene* lies on chromosome 11p15.5 and encodes for cathepsin D (CTSD or catD), the major lysosomal aspartic protease. CTSD is synthetized as an inactive preproenzyme (53 kDa), translocated to the ER compartment and modified post-translationally by glycosylation in an intermediate proenzyme form of 47 kDa. Finally, this proenzyme is sorted to lysosomal compartment, where it becomes functionally active by cleavage into two chain of 34 and 14 kDa that remain associated together by hydrophobic interaction. The CTSD substrates are not well characterized *in vivo* so far, although several studies suggest that CTSD is able to catalyze the hydrolysis of certain shingolipids and pro-saposins (Benes et al, 2008). Moreover, CTSD is involved in many biological processes, including cancer progression, antigen presentation, regulation of plasma HDL-C levels and caspase-independent apoptosis (Johansson et al, 2003; Zaidi et al, 2008).

Mutations in *CLN10* lead to a congenital NCL, the most severe NCL form with seizures and respiratory insufficiency at birth and early fatal outcome (Siintola et al, 2006; Steinfield et al, 2006). Residual activity of the enzyme is nearly absent in the infantile form, whereas relativly high residual activity in the rare juvenile phenotype (Steinfeld et al, 2006). The main stored material is SAP D but not SCMAS, resembling similar storage of infantile NCL. Sheeps, dogs and mouse with mutations in *CLN10* resemble the severity of NCL phenotype observed in humans beings and are useful animal model for the studies of these disorders.

CLNx or orphan forms

In spite of the recent advances in NCL genetic knowledge in the last decade, 10-15% of NCL patients do not show mutations in the eight known NCL gene. The existence of these

‘CLNx’ or ‘orphan’ NCL cases indicates that other NCL genes have to be discovered yet (Jalanko and Braulke, 2009**)**.

Several animal model with mutations in different endo-lysosomal proteins, such as channel chloride family (ClC) members or cathepsin proteins (specifically, cathepsin B, L and F), resemble the clinical and histopathological features of NCL disease, indicating possible candidate genes that could be linked to the human orphan forms.

PATHOLOGICAL MECHANISMS AND CELLULAR RESPONSES IN NCL AND LSD

The molecular mechanisms underlying cell pathology in LSD and particularly in NCL have not been fully elucidated yet. The storage of undigested substrates does not explain *per se* the various negative effects affecting the survival of the cells, and of neurons in particular. Different putative mechanisms have been hypothesized, that could affect the lysosomal compartment either directly or indirectly. Specifically, a primary effect of the lysosomal dysfunction is the formation of the storage. The presence of indigested material may engulf and induce topological distortion of the cell or could be *per se* a toxic factor. Then, any impairment of the lysosomal molecular degrading pathway could trigger an autophagic response in order to eliminate the storage material and to ameliorate the lysosomal stress. Moreover, lysosomal impairment could lead to secondary events that affect different compartments of the cell, such as ER, mitochondria and plasma membrane. Eventually, all these events together may exert negative effects on cell viability and affect cell survival, triggering the cell death process through several mechanisms, including apoptosis.

Many different animal models have been used in order to unravel the mechanism underlying cell pathology in NCL and LSD. Furthermore, together with animal models, fibroblasts have been extensively used in the study of these disorders. It is important to say that fibroblasts are cells deeply different from neurons; in particular, they are more resistant and less vulnerable to cell death and thus they might generate bias in the study of pathogenetic mechanisms. However, they show several important advantages; for instance, they are simply available from patients and can be cultured in controlled conditions. Moreover, they can provide many information about the cross-talk among different cellular compartment and the effects due to lysosomal dysfunction, both in basal and stressful conditions. In addition, NCL fibroblasts store in the cytoplasm the same biochemical and ultrastructural material of the neuronal cells. Finally, fibroblasts represent a rapid model on

which test hypothetical 'therapeutic' strategies, in order to see if these treatments can rescue some cellular functions, such as in the case of chemical chaperons employed to alleviate ER stress (Wei et al, 2008; Dawson et al, 2010). So the use of fibroblasts is very useful to analyze the different cellular mechanisms and to make up a putative 'pathogenetic model' that can be translated into neuronal biology.

Storage and topological distortion

The progressive accumulation of undegraded stored material causes a 'steric' engulfment of the cytoplasm of the cells, overwhelming the cell volume and perturbing indirectly the organization of other cellular compartments. In neurons, different morphological changes have been related to lysosomal diseases since early studies. For example, the formations of abnormal structures in axons, such as ectopic dendritogenesis and 'spheroid', have been described in different LSD (Vellodi, 2005; Walkey, 2009). These phenomena are respectively enlargements of axon hillock and aberrant swelling of the axons, that seem to be strictly connected to both primary or secondary gangliosides accumulation. However, the scenario is more complex since different neurons could be differently affected by these events. For examples, ectopic dendritogenesis interest usually a subset of cortical pyramidal neurons and GABAergic neurons, whereas Purkinje cells appear to be more vulnerable to spheroid formations (Walkley, 2009; Vellodi, 2005).

Storage and involvement of cell organelles

A lysosomal deficiency could secondarily affect other cellular compartments. For instance, ER has been reported to be involved in many LSD (Wei et al, 2008). Several proteins implicated in the unfolding protein response (UPR) exhibited high level of expression both on NCL and non NCL diseases and the use of chemical chaperones seems to alleviate the ER stress. In addition, also Ca^{2+} homeostasis appear to be altered in different LSD, probably as a consequence of alteration in the ER membrane composition that affect the capability of this cellular compartment to control the Ca^{2+} concentration (Walkley, 2009).

Moreover, several studies suggest that the mitochondrial compartment could be secondarily involved in different LSD. Accumulation of dysfunctional mitochondria has been reported in a multiple sulfatase deficiency (MSD) mouse model, both in neuronal cortex and in embryonic fibroblasts (MEF) (Settembre et al, 2008). Moreover, several studies on fibroblasts derived from mucolipidosis type IV (MLP IV) patients and on

astrocytes from a G_{M1} mouse model demonstrated that mitochondria exhibited both morphological and functional abnormalities, such as decreased membrane potential and reduced Ca^{2+} buffering capability (Vergarajauregui et al, 2008; Jennings et al, 2006; Takamura et al, 2008). Furthermore, mitochondrial involvement has been also investigated in NCL. Visual impairment is common clinical manifestation in NCL and also in other LSD. It is noteworthy that neurons of layer IV of visual cortex, highly dependent on oxidative metabolism, are particularly vulnerable to cell death. Moreover, it is known that the main storage material detected in cytosomes is the subunit c of ATP synthase, except for CLN1 and CLN10. Mitochondria showed morphological alterations (such as cristae abnormalities) in different human and ovine NCL fibroblasts (Jolly et al, 2002). In addition, the complex II and IV of respiratory chain and the ATP synthase activity have been reported to be compromised both in human and animal NCL fibroblasts, but in different manner according the different NCL forms (Das et al, 1999**)**. These findings imply the question whether an 'energetic imbalance' could be involved in NCL pathology. However, it is still matter of investigations whether the mitochondrial involvement might reflect a secondary energetic dysfunction related to lysosomal impairment, and therefore have relevant implications in NCL pathogenesis.

Storage and unbalance of degrading pathways: role of autophagy

As outlined before, lysosomes are key-organelles involved in many different degrading and recycling pathways of the cells. So, alterations in lysosomal function affect not only the degradation of particular substrates but also the recycling of different cellular components. Thus, for instance, the dysfunction in the digestion and recycling of different lipids and glycoproteins could lead to perturbation of lipid rafts, specific membrane regions implicated in many important process of the cell, such as signalling transduction (Walkley and Vanier, 2009). As regards neurons, it has been demonstrated that impairment on endo-lysosomal system affect vital pathways for neuronal function, such as AMPA receptor recycling and growth factors uptake (Walkley and Vanier, 2009; Walkley, 2009).

On the other side, also the presence of stored material could represent *per se* a toxic stimulus that cell tries to erase throughout autophagic pathway. Several LSD mouse models, such as mucopolysaccharidoses type IIIa (MLP IIIa) and MSD mice (Settembre et al, 2008), have demonstrated that an autophagic impairment, due to a lysosomal deficiency, could lead to the accumulation of indigested material, polyubiquitinated proteins, aberrant mitochondria and finally to neurodegeneration. With regard to NCL,

CLN3 deficient mice show storage of immature autophagic vacuoles and an increase of LC3 II in brain samples, suggesting a dysfunction of autophagic process (Cao et al, 2006). However, treatment *in vitro* with rapamycin, an inducer of autophagy, fail to increase cell survival of cerebellar cultures, whereas treatment with 3-methyladenine (3-MA), a blocker of autophagy, induce much more cell loss as compared to control. This result indicates that autophagy acts probably as a pro-survival pathway in CLN3-deficient mouse and the block of this process could increase the cell death. Moreover, also cathepsin-deficient mice (particularly, knock out for cathepsin D and double knock out for cathepsin B and L) exhibit increased levels of LC3 II marker and storage of double membrane vacuoles in both perikarya and axons of neuronal cell (Koike et al, 2005). In addition, increased LC3 II level are also detected not only in the brain, but also in liver and the heart, suggesting that the autophagic impairment is a condition common to different organs. Evidences of autophagic implications have also been suggested on human samples, such as the cytoplasmatic vacuolization detected on peripheral tissues (as well as neurons) of CLN3 patients, and the recent demonstration of large single membrane vacuoles also on CLN6 human biopsies (Cannelli et al, 2009). To date, it is not clear if autophagy represents just a rescue pathway or may be a negative mechanism for cell survival.

Storage and cell death

The relationship between lysosomal dysfunction and cell death is far to be clearly understood. As mentioned above, many different pathological events could arise in the cell and probably the single alteration is not *per se* a deadly trigger. Interestingly, two-thirds of LSD, including NCL, are marked by an extensive neuronal cell loss. The putative cellular mechanisms underlying this process are undoubtedly fascinating, but poorly characterized so far. The neuronal ‘deadly stimulus’ seems to be a ‘chronic’ stimulus, because LSD patients are normal at birth and neurons apparently survive for years until the onset of the early clinical symptoms. So it is likely that neuron degenerate in a progressive but not acutely manner, even though several clinical events, such as seizures in NCL, speed up this deadly process.

Many different experimental models have been employed so far in order to understand which mechanisms outline the extensive and selective neurodegeneration occurring in NCL but this matter is still controversial and debated. Several mouse model and few human studies suggest a causative role of apoptosis in NCL pathogenesis.

Apoptosis, term coined by Kern in 1972 (Kerr et al, 1972) to indicate a programmed cell death (in the same way as the "dropping off" of leaves from trees), is marked by specific morphological and biochemical features (Kroemer et al, 2009). It is noteworthy that apoptosis could be associated with or without caspases activation (so called caspase-dependent or independent apoptosis) and that several routes starting from different cellular organelles (such as ER, plasmatic membrane, mitochondria or lysosomes) could elicit apoptotic cell death (Ferri and Kroemer, 2001). Since different cellular compartments might be primary and secondarily involved in NCL and LSD, apoptotic pathway could be triggered in these disorders.

As regards NCL, it has been showed that in *ppt1* $^{-/-}$ mouse the activation of UPR system could lead to the apoptotic cell death through the ER-resident caspase-12 and the effector caspase-3 (Zhang et al 2006; Kim et al, 2006). Moreover, in the same mouse model the mitochondrial compartment could contribute to neurodegeneration by caspase-9 and oxidative stress (Kim et al, 2006). In addition to these evidences on mouse model, human NCL fibroblasts show higher level of cell death induced by brefeldin A, a chemical inducer of ER stress, and the use of chemical chaperones is able to reduce the cell death in this *in vitro* model (Wei et al, 2008). Furthermore, in neuroblastoma cell lines, PPT1 overexpression seem to protect from apoptosis induction (Cho and Dawson, 2000), whereas the inhibition of PPT1 transcription, by using antisense oligonucleotides treatment, increases the apoptotic cell death (Cho et al, 2000).

Notwithstanding these evidences of an apoptotic involvement in genetically different NCL forms, several studies suggest that other mechanisms leading to cell death have to be taken into account to explain NCL-related neurodegeneration. In particular, PPT1 and TPP1 deficient fibroblasts show decreased sensitization to TNF alpha-induced apoptosis, whereas CLN3 and CLN5 deficient fibroblasts do not exhibit a similar behaviour (Tardy et al, 2009, Autefage et al, 2009). Only the enzymatic correction through PPT1 gene transfection is able to restore the susceptibility to TNF apoptotic induction. Moreover, double knock out mice, which harbour mutations in a NCL and apoptosis-related genes at the same time, have demonstrated that neurodegeneration is still present, even though the apoptotic pathway lacks important factors, such as BAX (Shacka and Roth, 2007; Shacka et al, 2007). Moreover, over-expression of Bcl-2 or knock out of p53 fail to modify the lifespan of CLN2 $^{-/-}$ mouse model, suggesting that the apoptotic pathway, depending at least from Bcl-2 and p53, is not directly involved in the disease progression (Kima et al,

2009). Taking together, these findings suggest that apoptosis is not the only mechanism that might explain the cell death in NCL.

Probably, other cellular responses, such as an increased autophagic response, might be also deleterious for cell survival and trigger the cell death. Impaired feed-back mechanisms which should regulate the physiological, rescue process of autophagy, for instance, might lead to extensive cytoplasmic vacuolization, which deadly impairs cytoplasmic activities, leading eventually cells to die (by autophagic cell death type II).

4. AIMS OF THE DOCTORATE PROJECT

NCL are a heterogeneous group of neurodegenerative disorders of childhood, classically considered as "lysosomal disorders". They are caused by mutations on genes codifying for proteins that resides on different cellular compartments, including lysosomes. NCL are often accounted as precocious 'aging' diseases due to the premature and progressive accumulation of lipofuscin and indigested material in neuronal tissue, leading to progressive cognitive decline and premature death. To date it is still not clear whether the storage material could be *per se* deleterious for the survival of neurons or may trigger unbalanced cellular responses (such as autophagy and apoptosis) that eventually lead to cell death.

The aim of my doctorate project was to study *in vitro* the cellular behaviours of human NCL fibroblasts in order to possibly recognize any pathogenetic mechanisms that could be involved in some NCL forms. Specifically, we employed genetically determined human fibroblasts cell lines belonging to different NCL forms, with 'primary' (CLN1) and 'secondary' (CLN3, CLN5, CLN6 and CLN7) lysosomal involvement.

Fibroblasts were analyzed in a 'prolonged culture paradigm' (under basal conditions and following specific stresses) in order to assess whether the cellular aging could exacerbate the pre-existing endo-lysosomal dysfunction and influence the cellular survival.

In particular, we studied the process of lysosomal bodies accumulation and the mechanisms by which cell try to cope with the endo-lysosomal stress, caused by both genetic alteration and the long-lasting growth. Likewise, we examined whether the endo-lysosomal system could influence the spatial topology and the function of mitochondria, a cellular compartment essential for cell viability. Finally, we tried to understand whether the endo-lysosomal stress could induce cell death, focusing mainly on the caspase dependent apoptotic pathway.

Therefore, the main topic was the study of the endo-lysosomal system and the morphological changes that affect this compartment during the long-lasting growth. For this purpose, we employed three different approaches: *in vivo* visualization of the acidic compartment using Lysotracker probe, immunofluorescence assay against Lamp2 (a lysosomal membrane protein) and the electron microscopy analysis. Taken together, these methodologies allowed us to follow up the distribution of acidic structures in the cells, to detect lysosomal-derived vesicles and finally to characterize their ultrastructural features. At the same time, we investigated the autophagic process by immunoblotting and

immunofluorescence analyses of two main biochemical markers, the Atg12-Atg5 complex and LC3 II, with the support of the ultrastructural analysis.

Moreover, we studied the involvement of mitochondrial compartment in NCL, focusing on the spatial relationship between mitochondria and endo-lysosomal system and on the functional alteration of both polarization state of mitochondrial membrane and respiratory chain. Finally, we put our attention on the apoptotic process, by investigating two late steps of the caspase-dependent apoptotic pathway, cleavage of caspase-3 and nuclear fragmentation, both under basal condition and following chemical induction with Staurosporine.

5. MATERIALS AND METHODS

Human fibroblast cultures

Primary fibroblasts cultures were established from skin biopsy of healthy donors and NCL patients. Human fibroblasts were cultured in Dulbecco's Modified Essential Medium with high Glucose (DMEM/HIGH Glucose, EuroClone) supplemented with 10% foetal bovine serum, penicillin (50 IU/ml), streptomycin (50 µg/ml) and amphotericin B (250 µg/ml) (all purchased from EuroClone). Cells were incubated at 37°C in a humidified air with 5% CO_2. The medium was changed twice a week. At confluence, cells were detached from the flasks with trypsin/EDTA (Sigma-Aldrich) and subcultured at the same density for all the cell lines.

In table 2 a list of NCL fibroblast cell lines employed in this study is shown. Four fibroblast lines established from healthy children donors were used as normal controls.

NCL and control fibroblasts were analyzed at different stages of culture in a long lasting paradigm. In particular, considering the isolation of fibroblasts from biopsy as the first passage, the experimental evaluations were set at three different culture points, the 7^{th}, 15^{th} and finally 20^{th} passages, corresponding to "early" and "late" stages of culture respectively.

For fluorescence and light microscopy analysis, at the established passages, cells were seeded on round glass coverslips in a 24-well plates (2000 cell per well) and cultured in complete medium for 48 or 72 hours until the day of experiment.

Visualization of mitochondrial and lysosomal compartments by vital fluorescent dyes

We employed two different fluorescent probe, Mitotracker and Lysotracker (Molecular Probes) with the aim to study mitochondrial and lysosomal compartments respectively. Specifically, NCL and control fibroblasts, grown on coverslips, were exposed to the specific fluorescent dyes (100 µM Mitotracker Red or Green, 50 nM Lysotracker DND 99) for 30 minutes, at 37°C 5% CO_2, then rinsed in PBS and observed immediately under Axiolab microscope (Zeiss) for incident-light fluorescence, equipped with HBO 50 mercury vapour short-arc lamp. Nuclei were counterstained with 2 µM Hoechst 44432 (Molecular Probes). Moreover, to analyze the spatial relationship between mitochondrial network and lysosomal compartment, cells were contemporarily exposed to 100 µM Mitotracker Green and 50 nM Lysotracker DND 99 (Molecular Probes) at the same conditions described previously. Images were acquired by an AxioCam equipment using

Cell Line	Clinical form	NCL Gene	Nucleotide alteration	Mutation	Predicted effect on protein
CLN1 -1	vINCL	CLN1	c.541G>T c.124+1214	Missense 3.6 kb deletion	p.Val181Leu Multiple exon skipping
CLN1 -2	vLINCL	CLN1	c.665T>C	Missense	p.Leu222Pro
CLN1 -3	cLINCL	CLN1	c.A169-170insA	1 bp insertion	Framshit after k56
CLN1 -4	vLINCL	CLN1	c.125-15T>G	Splice site	Aberrant splicing
CLN3 -1	JNCL	CLN3	c.462-677del	1.02 Kb deletion	Frameshift after C153
CLN3 -2	JNCL	CLN3	c.462-677del c.222+2T>G	1.02 Kb deletion Splice site	Frameshift after C153 Aberrant splicing
CLN5	vLINCL	CLN5	c.772T>G	Missense	p.Tyr258Asp
CLN6 -1	vLINCL	CLN6	c395delCT c.715delTTCG	2-bp deletion Nonsense	p.Asp132CysfsX17 p.F238fs
CLN6 -2	vLINCL	CLN6	c.406C>T c.426C>G	Missense Nonsense	p.Arg136Cys p.Tyr142X
CLN6 -3	vLINCL	CLN6	c.316insC	1-bp insertion	p.Arg106ProfsX26
CLN7	vLINCL	CLN7	c.154G>A c.863+3insT	Missense 1-bp insertion	p.Gly52Arg Altered splicing

Table 2.
NCL fibroblasts cell lines and related mutations employed in this study.

AxioVision 4.3 software (Carl Zeiss). The image acquisition settings were established and maintained identical in all the experiments. Moreover, in order to investigate the alteration of the mitochondrial reticulum linked to lysosomal engulfment, we performed a semi-quantitative analysis, determining the percentage of cells that showed a fragmented or distorted reticulum after Mitotracker staining. Cells were arbitrarily divided into two groups, cells with normal and filamentous mitochondrial network and cells with fragmented and discontinuous reticulum. The percentage of cells belonging to each group was determined and compared to controls.

Mitochondrial membrane potential (Δψm)

To investigate the state of polarization of mitochondrial membrane (Δψm), fibroblasts were exposed to JC-1 (5,5',6,6'-tetrachloro1,1',3,3'-tetraethylbenzimidazolyl carbocyanine, Molecular Probes) for 30 minutes at 37°C, 5% CO_2, at the final concentration of 10 µg/ml in a specific medium with high K^+ concentration (137 mM KCl,

3.6 mM NaCl, 0.5 mM $MgCl_2$, 1.8 mM $CaCl_2$, 4 mM HEPES, pH 7.2, with 1 mg/ml D-gluscose). The sample was analyzed by Axiolab microscope and images were acquired in the same way as for Lysotracker and Mitotracker. JC1 localizes to mitochondrial membrane and changes its molecular conformation according to the $\Delta\psi m$. In particular, for high $\Delta\psi m$, JC-1 forms dimeris and displays red fluorescence; on the other side, when $\Delta\psi m$ is impaired, JC-1 is present as monomer, emits green fluorescence and could be released in the cytoplasm.

Immunofluorescence assay

Fibroblasts, grown on coverslips, were fixed in Methanol at -20°C for 10 minutes or alternatively in Methanol: Acetone 1:1 for 10 minutes at RT. After two washing in PBS, cells were blocked with 10% Normal Goat Serum (Dako) with the addition of 1% BSA (Sigma-Aldrich) and then incubated with primary antibodies over night at 4°C. Anti-Mouse and Anti-Rabbit Alexa Fluor 488 and 594 (Molecular Probes) were used as secondary antibodies for 1 hour RT and the nuclei were counterstained with 4',6-diamidino-2-phenylindole dihydrochloride (DAPI, Sigma-Aldrich). Primary antibodies used in this study for immunofluorescence were monoclonal anti-Lamp2 (H4B4 clone; Abcam), polyclonal anti-LC3B (direct against amino-terminus region of the protein; Cell Signalling Technology) and polyclonal anti-cleaved caspase-3 (able to recognize amino-terminal residues of the cleaved form but not the full length protein; Cell Signalling Technology).

Electron microscopy

Lysosomal compartment and mitochondria were examined by transmission electron microscopy (TEM). Briefly, fibroblasts at confluence in a T75 flask were collected by trypsinization, and centrifuged at 150 g, washed with HBSS (EuroClone) and finally in phosphate buffer. Cells were then fixed with 1.25% glutaraldheide and 0.5% paraformaldeide in phosphate buffer for 1 hour at 4°C and post-fixed in osmium tetraoxide (OsO4) for 2 hours at 4°C. Cellular pellet was subsequently dehydrated by increasing concentrations of acetone and included in Spurr resin.

For lysosomal compartment examination, at least two hundred of control and NCL fibroblasts were observed and checked for the presence of vacuoles or lysosomal bodies. For every single cell, a score was assigned, referring to the subjective evaluation (by two independent observers) of vacuoles and lysosomal bodies per cell.

For mitochondrial density analysis, at least 10 images of nucleated cells were acquired at 3000X magnification. The EM photographs were acquired by a scanner at 600 dpi resolution and then analyzed by AxioVision 4.3 software. Mitochondria were counted within a total cellular area of roughly 300 μm^2. We considered as mitochondria only those organelle that showed a clear double membrane with a unambiguous matrix and cristae inside.

Western blot analysis

Fibroblasts were collected from a T75 at confluence, washing twice with PBS and then resuspended with RIPA Buffer (150 mM NaCl, 50 mM Tris-HCl, 6 mM EDTA, 1% NP-40, 1% SDS, 0.5% Deoxycolic acid, pH 8.0) containing protease inhibitors (Roche Diagnostics). After 2 hours of homogenization at 4°C, homogenates were centrifuged at 3200 g to discard cellular debris and then the supernatant was collected and stored at -80°C. Protein content were determined by Bradford Assay (Sigma-Aldrich). For western blot analysis, twenty micrograms of total protein lysates were diluted in Laemli buffer, boiled at 90°C for 5 minutes and then resolved by electrophoresis in SDS-polyacrylamide gels under denaturing conditions. Proteins were then electrontransferred to nitrocellulose membrane (Bio-Rad). The membranes were blocked with TBS/0.1% Tween20 containing 10% non-fat dry milk (Bio-Rad) and then subjected to immunoblot analysis. Primary antibodies were incubated over night at 4°C in TBS/0.1% Tween20 with 5% non-fat dry milk. The secondary antibodies, anti-Mouse IgG HRP or anti-Rabbit IgG HRP (Amersham GE Healthcare), were added for 1 hour at RT in the same buffer of primary antibodies. Chemiluminescent detection was performed with ECL Plus (Amersham GE Healthcare) according to manufacturer's instructions. Quantitative blot analysis was performed by ImageJ software (NIH). Primary antibodies used for western blotting analysis were the anti-LC3 antibody previously described, the polyclonal anti-Atg12 (that recognizes a peptide near the amino terminus and allows the detection of the Atg12-Atg5 complex, corresponding to a 53 kDa band; Cell Signaling Technology) and polyclonal anti-VDAC (direct against amino terminus of the human VDAC-1; Cell Signalling Techonology) antibodies, and the monoclonal anti-COX IV (clone 20E8C12; Mitosciences) antibody. Polyclonal anti-Actin (that probes a N-terminal conserved region of the protein; Sigma-Aldrich) and monoclonal anti-α tubulin (that recognizes a N-terminal domain; Invitrogen) antibodies were employed as quantitative loading control.

Biochemical assay respiratory chain

Enzymatic activity of respiratory chain was evaluated biochemically. Fibroblasts from 1 or 2 T75 at confluence were washed and collected in NaCl-Tris Buffer (140 mM NaCl, 35 mM Tris/HCl, pH 7.4), then cells were resuspended in 300 µl of homogenization buffer (250 mM sucrose, 10 mM Tris/HCl and 2 mM EDTA, pH 7.4) and sonicated twice at 40% power for 5 seconds. Finally, the lysate was diluted 1:2 with other 300 µl of homogenization buffer and Triton X100 (Sigma-Aldrich) was added at final concentration of 0,01%. Samples were incubated on ice for 30 minutes and then the activites of the mitochondrial enzymes Cytochrome c Oxidase (COX), NADH Cyt, Succinate Dehydrogenase (SDH), Succinate Cytochrome c Reductase (SCR) and NADH Dehydrogenase (NADH DH) were evaluated following incubation at 37° C for 5 minutes, as previously described (DiMauro et al, 1987). Enzymatic activity was given as nmol/min/mg protein and corrected for the Citrate Synthase (CS) activity that represents an index of the 'mitochondrial mass'.

Apoptosis evaluation

To assay apoptotic cell death in control and NCL fibroblasts, nuclei morphology and caspase-3 activation were analyzed. In particular, nuclei with apoptotic morphology were evaluated by DAPI fluorescence, while cleavage of caspase-3 was assessed by both immunofluorescence and western blot analysis. Moreover, in order to induce apoptosis, cultures were exposed to 500 nM Staurosporine (STS, Sigma-Aldrich), a protein kinase inhibitor, for 16 hours. Such experimental paradigm was chosen following a pilot study (see addendum 1). The same number of cells was plated, to evaluate differences in decreased cell density among control and NCL fibroblasts after treatment. For quantitative analysis, the number of cleaved caspase-3 positive cells and of fragmented nuclei were obtained after scanning under the microscope the seeded plates. For each cell line, figures of the remaining cells after STS treatment were compared to untreated cells and differences among cell population were given as percentage.

BrdU incorporation assay

To evaluate the proliferation of control and NCL affected fibroblasts, we carried out a BrdU incorporation assay. BrdU is an analogue of the dC nucleotide and is incorporated in DNA of cells during S phase of mitotic cycle. After 72h of culture on coverslips, cells were

exposed to 10 µM BrdU (Sigma-Aldrich) in complete medium for 5 hours and then fixed in Methanol at 4° for 10 minutes. DNA was denatured with 2N HCl at 37°C for 1 hour, then the coverslips were neutralized in $Na_2B_4O_7$ (0.1 M, pH 8.5), washed in PBS and blocked with 10% Normal Goat Serum for 30 minutes. Primary antibody incubation was performed over night at 4°C with monoclonal mouse α-BrdU (Sigma-Aldrich) in PBS with 1% BSA and 0.5% Tween20. BrdU-labelled cells were visualized with Goat α-mouse Alexa Fluor 488 (Molecular Probes) and nuclei were counterstained with DAPI. Percentage of BrdU labelled cells was given as number of nuclei BrdU-positive on number of DAPI-staining nuclei.

Statistical analysis

Statistical significance were determined by t-student test analysis. A p value minor to 0.05 was considered as significant, whereas a p value minor to 0.01 was considered as highly significant.

Addendum 1

We performed a pilot study to determine the optimal conditions for Staurosporine treatment in order to assess possible differences in the activation of the caspase-3 dependent apoptotic pathway between NCL and control fibroblast cultures. For this preliminary experiment, we employed a control (C2) and CLN1-1 cell lines at early passages of cultures (8^{th} passage). Cells were seeded at the same density and after 72 hours were exposed to the apoptotic inducer at different conditions. The number of the cleaved caspase-3 positive cells and fragmented nuclei were counted after immunofluorescence assay and given as percentages on the remaining cellular population. Coherently, fragmented nuclei co-localized with the caspase-3 positive cell, so the percentages of caspase-3 positive cells and percentage of fragmented nuclei were homologous. For this pilot study, only one dish was counted, so we could not perform a statistical analysis.

1 µM STS is usually employed to induce apoptosis *in vitro*. Previous works have already showed high values of cleaved caspase-3 enzymatic activity after both 8 and 16 hours treatment, using a STS concentration lower than 1 µM (in particular 100 nM; Johanssonn et al, 2003). Likewise, we decided to use a concentration minor to 1 µM in order to asses if NCL fibroblasts were more vulnerable to the caspase apoptotic cell death as compared to controls at low concentration of STS.

For these reasons, we analyzed control and CLN1 fibroblasts after exposure to 50 nM and 500 nM for 4, 8 and 16 hours. After 4 hours, fibroblasts changed their morphology and began to shrink, but no fragmented nuclei or cleaved caspase-3 positive cells were detected at this time (data not shown).

After 8 hours, a significant cell density reduction was reported and low percentages of fragmented nuclei and apoptotic cells were measured, according to the different STS concentrations (figure 2). After 16 hours, the exposure to 50 nM STS induced low amount of apoptotic cells, whereas at the concentration of 500 nM higher percentage of fragmented nuclei and cleaved caspase-3 positive cells were evident.

Therefore, this pilot study indicated that in our model the best STS treatment conditions were 16 hours exposure to a concentration of 500 nM. Indeed, using this paradigm, we were able to measure a significant percentage of fragmented nuclei and cleaved caspase-3 positive cells and we could also analyzed the different cellular response between NCL and control lines, as regard the caspase-3 dependent apoptotic pathway.

A

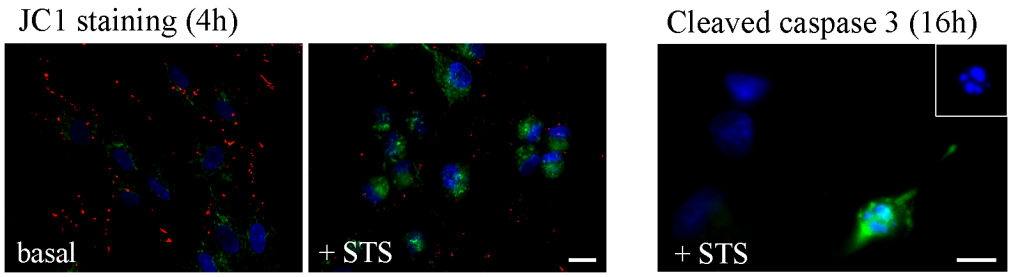

B

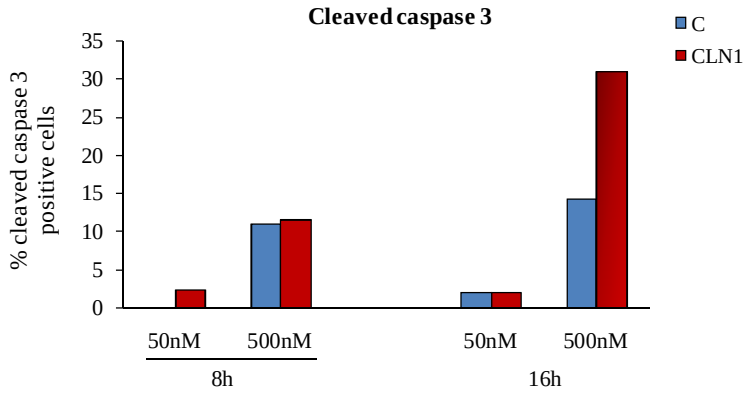

Figure 2 .

Apoptotic cell death investigation in NCL fibroblasts.

A. After 4 hours of STS exposure dots of JC1 staining are present in the cytoplasm of shrunken CLN1-1 fibroblasts (left). At this time no fragmented nuclei are detected. After 16 hours of exposure to 500 nM STS, cleaved caspase-3 positive cells with fragmented nuclei appear (right). Nuclei were counterstained in blue with Hoechst (left) or DAPI (right); scale bars equal to 10 µm.

B. Increased amounts of cleaved caspase-3 positive cells following STS treatment at different concentrations (50 and 500 nM) and time exposure (8 and 16 hours). Markedly evident different behaviour between control (C2) and CLN1-1 fibroblasts are evident at 500 nM STS concentration, following 16 hours of exposure.

6. RESULTS

The first issue addressed in this thesis was the evaluation of the endo-lysosomal compartment behaviour along time, namely the differences among control cells and different NCL fibroblast lines. Then we investigated the process of autophagy, as a major mechanism of the cells to cope with the abnormal storage. The effects of abnormal storage on the mitochondrial reticulum and related functions was then examined even to search for evidences of apoptotic cell death in this experimental paradigm.

THE ENDO-LYSOSOMAL COMPARMENT

Cell behaviour as regard to the lysosomal bodies formation along time

Control Fibroblasts

At early passages, fibroblasts showed typical 'spindle-shape' profiles and had good proliferation ability. Lysotracker positive 'dotted' vesicles could be detected over the cytoplasm, both near nucleus and in the cell periphery (figure 3). The Lamp2 staining pattern and distribution resembled Lysostracker staining and indicated the presence of small lysosomal vesicles distributed in the cytoplasm of the cell. Moreover, the ultrastructural examination revealed that lysosomal structures were prevalently 'electron-dense' lysosomal bodies, whereas only few single membrane empty vacuoles could be detected. At 15-18th passages, the staining pattern of the endo-lysosomal structures changed significantly. In particular, Lysotracker and Lamp2 immunofluorescence was enhanced and spread all over the cytoplasm, suggesting an increased density and distribution of these structures (figure 3 and 4). The expansion of the endo-lysosomal compartment affects directly the cellular morphology: several fibroblasts became larger, increased in size and lost their typical 'spindle-like' shape. In addition, the proliferation rate of these aged cultures decreased and cells grew slowly. The ultrastructural analysis, as expected, confirmed the increased amount of lysosomal organelles of different morphology, whereas only few vacuolated cells were detected. Thus, in the control fibroblasts the accumulation of lysosomal structures, the loss of characteristic shape and the reduced proliferation capability are the main features that characterized the prolonged growth of the control fibroblast and they are the cell morphological features related to the aging of these cultures.

NCL Fibroblasts

The same morphological analysis was performed on different genetically determined NCL fibroblasts. NCL lines showed different behaviours of the lysosomal compartment according to time and NCL form.

Lysotracker and Lamp2 immunofluorescence showed an expansion of the lysosomal

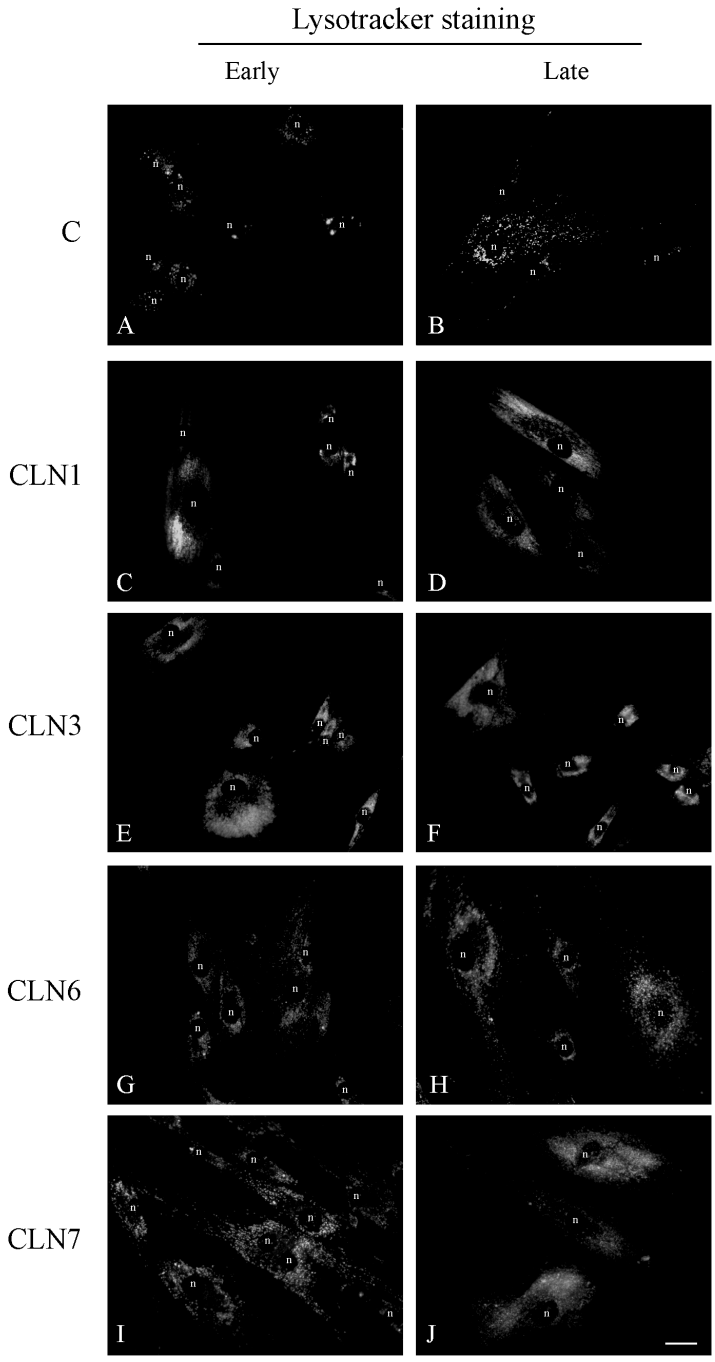

Figure 3.

Lysotracker staining of control and NCL lines during the prolonged culture.

Punctated pattern is seen in control fibroblasts at early passages (A), whereas this pattern is diffuse over the cytoplasm at later stages (B). Conversely, the acidic compartment is diffusely and markedly stained in all NCL lines at early stages (C, E, G, I). At late passages, many cells appear swollen and even brighter, engulfed with endo-lysosomal material (D, F, H, J). Scale bar equal to 20 µm; n: nucleus.

compartment and an abnormal distribution of lysosomal vesicles in NCL fibroblasts since the early passages (figure 3). In particular, Lysotracker and Lamp2 immunofluorescence suggested that many more lysosomal vesicles (as compared to controls) engulfed the cytoplasm of NCL fibroblasts, forming tightly related storages mainly in the perinuclear region. The engulfment with lysosomal material affected the cellular morphology; Lysotracker positive, swollen cells (particularly of specific NCL forms, such as CLN1, CLN3 and CLN7) could be observed since the early passages (figure 3). Along time this pattern became more evident, and at late passages the vast majority of NCL fibroblasts (independently from the form and the mutations) were swollen and overwhelmed by Lysotracker and Lamp2 positive structures. However, his phenomenon was always more evident in CLN1, CLN3 and CLN7 lines. Furthermore, CLN1 and CLN7 lines exhibited also a slowed growth, since the early passages, as detected by BrdU assay (data not shown).

Even the ultrastructural pattern of NCL fibroblasts showed variations among the different NCL forms, and was markedly distinct from the features of control cells. Since the early stages of cultures, NCL fibroblasts were characterized by the accumulation of lysosomal bodies, often closely related to empty vacuoles lined by a single membrane (figure 4); this feature was more impressive in the CLN3, CLN6 and CLN5 lines. These vacuoles were mainly optically empty and it was not possible to determine their origin precisely. However, the detection of Lamp-2 positive large vesicles by immunofluorescence suggests that most of these vacuoles are of lysosomal nature. This mixture of vacuoles and lysosomal bodies localized prevalently near the nucleus, resembling the same distribution depicted by Lysotracker and Lamp2 fluorescence.

Semiquantitative analysis of electron microscopy samples revealed a markedly increased evidence of lysosomes and dense bodies, which cannot be related to the cellular aging process of the cultures only. Furthermore, NCL fibroblasts in general exhibited a higher percentage of vacuolated cells as compared to controls, both at early and late passages of cultures. However, the behaviour of the NCL lines was not always homogeneous, because different patterns could be detected even within the same NCL form.

Specifically, the three CLN1 lines seemed to share a common trend. During the early stages the amount of dense bodies was not particularly marked and they were similarly scattered in the cytoplasms of the three cell lines; their morphological features were similar to those of controls. Along time a steady increase in the lysosomal component was observed. A meaningful increase of vacuolated cells was seen (about 50% of cells were

vacuolated), and the amount of vacuolization increased similarly in the three cell lines. The size of empty vacuoles that characterized the aging of CLN1 cultures was similar to the size of the dense bodies.

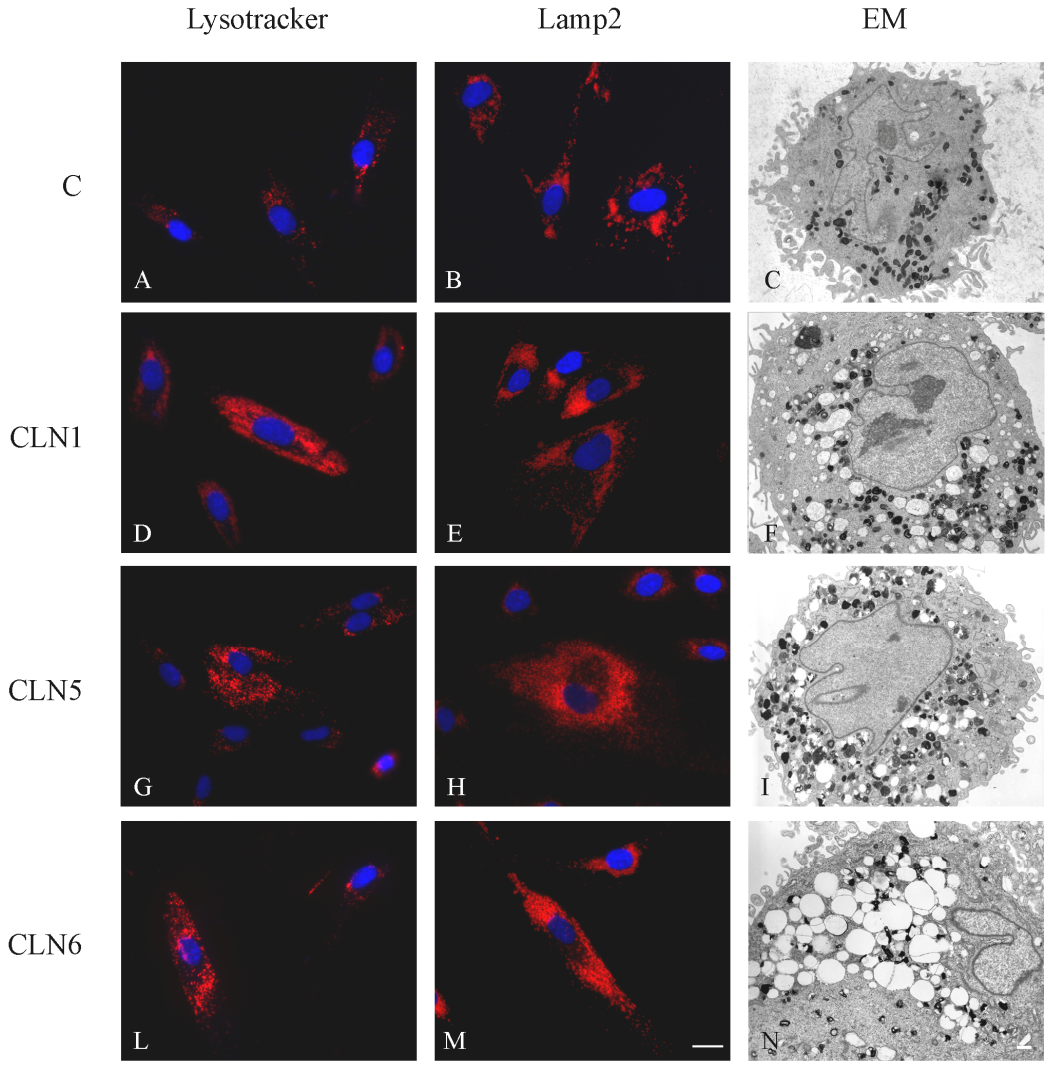

Figure 4.
Morphological analysis of the lysosomal compartment at 15th passage: Lysotracker staining (A, D, G, L), Lamp2 immunofluorescence (B, E, H, M) and electron microscopy (C, F, I, N). Blue fluorescence represents the Hoechst nuclear staining. Many NCL fibroblasts appear swollen and engulfed with fluorescent markers of endo-lysosomal compartment as compared to control. By electron microscopy, in NCL fibroblasts the lysosomal compartment appears to be made up of both vacuoles and lysosomal bodies. Scale bar for Lysotracker and Lamp2 images equal to 20 µm. Electron microscopy images were acquired at 3000x magnitude; scale bar equal to 1 µm.

Different patterns of cytoplasmic changes occurred in CLN3, CLN6 and CLN5 cell lines. In general, in these NCL forms, the dimension of the empty vacuoles were larger as compared to those of CLN1. Moreover, another distinct feature was the high number of lysosomal bodies enclosing partially digested cytoplasmatic material (probably, autolysosomes), that were detected in lower amount in controls and CLN1 lines.

As concern CLN3, both CLN3 lines showed high score of vacuolization at early observations, with a further increase of single cell vacuolization at later steps, whereas the marked increased of lysosomal bodies accumulation was seen of CLN3 -2 line only. The morphology of vacuoles in CLN3 fibroblasts were often associated with expanded endoplasmic reticulum cisternae. Moreover, double membrane structures, typical of autophagosomes, were detected in the cytoplasm of CLN3 -2 cell lines (figure 5).

With regard to CLN6, all three cell lines showed a meaningful progression of cells having cytoplasmic lysosomal bodies from early to late stages of culture, as well as the number of cells showing heavy dense bodies accumulation increased too. Different trends were observed as far cytoplasmic vacuoles are concerned: two lines (CLN6 -1 and -3) showed meaningful increase of vacuoles along time, as well as increased the number of markedly vacuolated cells. On the contrary an opposite trend was observed in CLN6-2, where dramatic reduction of vacuolated cells occurred. Furthermore, dramatically enlarged vacuoles were observed at the early observation in CLN6-2 only, and this pattern, however, was never seen at later stages (figure 5). In addition, autophagosomes were detected in two CLN6 lines at different stages of cultures, at both time steps (CLN6 -2) or merely at late passages (CLN6 -3).

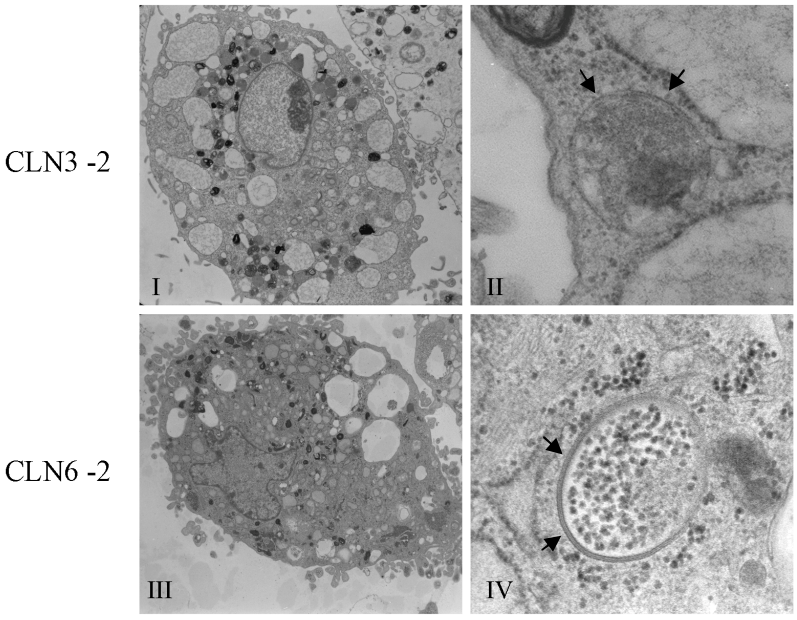

Figure 5.
Evidences of autophagy in CLN3 -2 (I and II) and CLN6 -2 (III and IV) at early passages. Ultrastructural detection of dramatically enlarged vacuoles (I and III) and double membrane autophagosome in the cytoplasm (arrows, II and III). Photos were acquired at 3000X (I and III) and 50000X (II and IV) magnitude.

Finally, CLN5 resembled the trend of CLN6 -2, with dramatic increase in lysosomal bodies and decrease of vacuoles from the early to the late stages of cultures. In particular, at early passages many empty vacuoles, both large and small, were detected, whereas at late passages the accumulation of many autophagolysosome, enclosing partially digested material, was prevalent.

Evidences of activated autophagic pathway

The morphological analysis of the endo-lysosomal system suggested activation and expansion of this compartment in the NCL cultures. The presence of many single membrane vacuoles at different time of observations in all NCL cell lines, as well as the ultrastructural evidence of double membrane layered autophagosomes, led us to investigate whether the cytoplamic vacuolization might be indeed expression of activated autophagic pathway. Thus, we analyzed the expression of two different proteins involved in autophagy, the cytosolic LC3 I/LC3 II complex and the Atg12-Atg5 complex, by means of indirect immunofluorescence and western blot.

Double staining with anti-LC3 and -Lamp2 antibodies revealed that many LC3 positive vacuoles were present in the cytoplasm of different NCL cell lines since early passages (figure 6 and table 3). Moreover, in the case of CLN3 -2 and CLN6 -2, the fluorescent

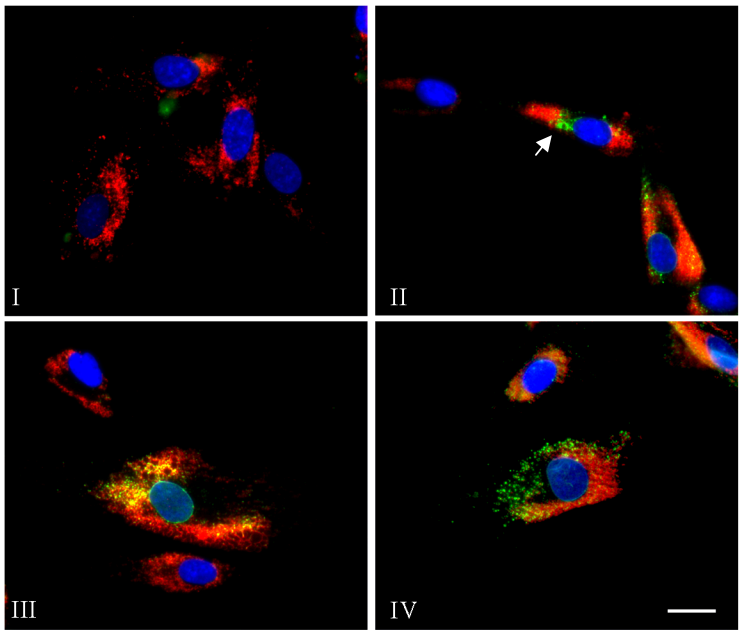

Figure 6.
Double immunofluorescence assay against Lamp2 (red) and LC3 (green) at early passages of culture. Nuclei are counterstained with Hoechst (blue). Lamp2 immunoreactivity fills the large majority of the cell body; LC3 II punctated fluorescence can be either independent from Lamp2 signal (II and IV) or partially merged (co-localization in yellow signal, III). 'Green' circle structures – presumably LC3 lined vacuoles – are detectable (arrow, II). (I, control; II CLN1-3; III CLN3 -2; IV CLN6 -2). Scale bar equal to 20 µm.

evidence of autophagosome formation was supported by the detection of autophagosomal-like structure at electron microscopy analysis (figure 5). On the other side, only few sporadic LC3 dots were detected in control cells. Moreover, many LC3 positive vesicles were detected also in the cytoplasm of CLN1 -3 and it was possible to see LC3 positive structures that resembled the morphology of vacuoles (figure 6, arrow).

As expected, the Atg12-Atg5 complex was expressed in both control and NCL fibroblasts without significant differences both at early and late stages of cultures (figure 7A).

As regards the western blotting analysis of LC3 isoforms, at early passages control cells did not show LC3 II expression, whereas different NCL fibroblast lines exhibited both the

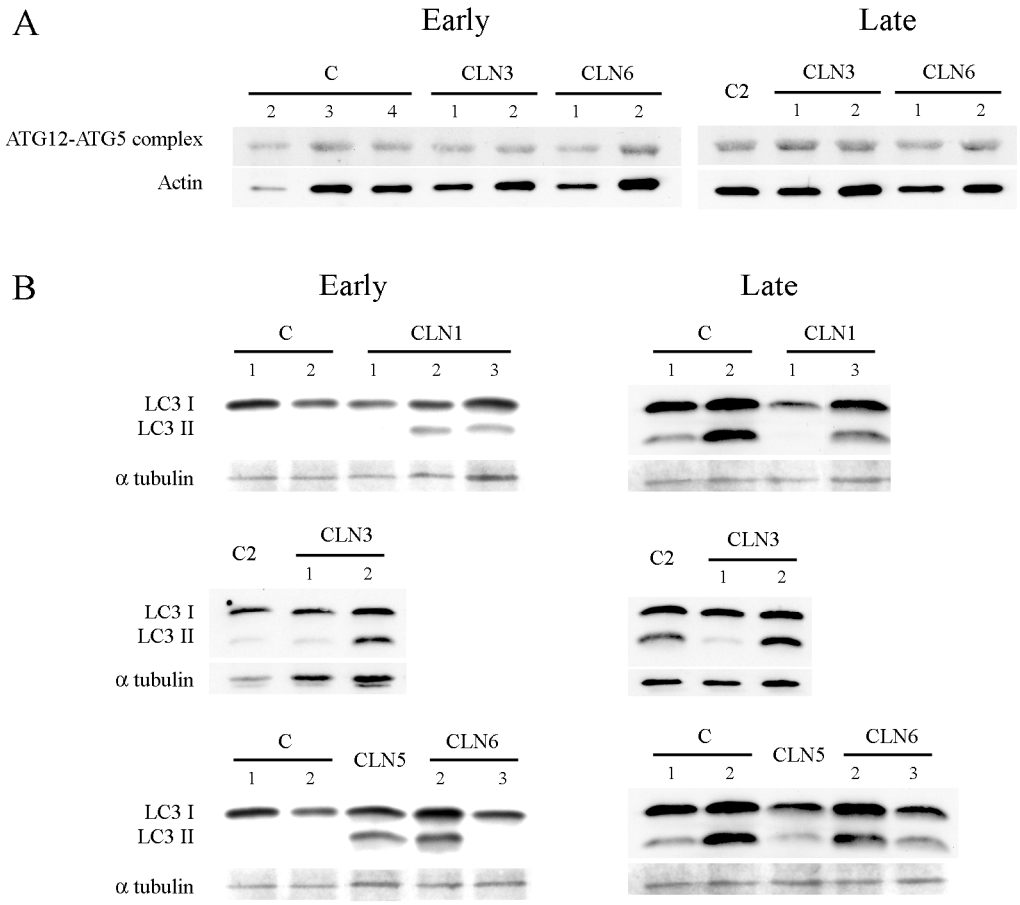

Figure 7.

A. Western blotting analysis of Atg12-Atg5 complex. The complex is expressed at same level in control and NCL fibroblasts, both at early and late stages of culture.

B. LC3 western blotting analysis on controls (C1 and C2) and different NCL lines, both at early (9-10th p) and late (16-18th p) stages of cultures. At early passages, LC3 II isoform is present, with different intensity, in CLN1 (lines 2 and 3), CLN3 -2, CLN6 -2, and CLN5, suggesting an activation of autophagic pathway in these NCL cell lines. At 16-18th passages LC3 II band is seen in control cells, is still present in CLN1 -3, CLN3 -2 and CLN6 -2, fades in CLN5 and is weakly present in CLN6 -3.

14 kDa and the 16 kDa bands (figure 7B). However, likewise the ultrastructural analysis of vacuoles and lysosomal bodies, NCL fibroblasts showed a heterogeneous behaviour in the expression of LC3 isoforms since differences among cell lines affected by the same NCL form could be found. In particular, CLN1-2 and CLN1-3 fibroblasts showed similar patterns of LC3 II expression (whereas no signal was seen in CLN1-1) (figure 7B). CLN6 -1 and CLN6 -3 cells did not show expression of LC3 II, whereas high levels were detected on CLN6 -2. In addition, CLN3 -2 exhibited high level of LC3 II, whereas CLN3 -1 showed a weaker signal. However, it is important to note that the western blot analysis of LC3 II always confirmed the detection of many LC3 positive vesicles following immunofluorescence assay in the same lines. Finally, the analysis on aged cultures showed LC3 II expression in control fibroblasts and differences as far as NCL cell behaviour. In CLN1 -3, CLN3 -2 and CLN6 -2 lines the pattern was still present, whereas the signal intensity decreased in CLN5 line. Eventually, the LC3 II isoform expression was never found in CLN3 -1 and CLN6 -2.

Results of the LC3 immunofluorescence assay related to the signal intensity on western blot are summarized in table 3.

	Early		Late	
	IF	**WB**	**IF**	**WB**
C1	-	±	±	+
C2	-	-	+	+++
CLN1 -1	+	±	+	-
CLN1 -2	++	++	+	nd
CLN1 -3	++	++	++	+++
CLN3 -1	nd	±	±	-
CLN3 -2	+++	+++	+++	+++
CLN5	+	++	+	+
CLN6 -1	nd	-	±	-
CNL6 -2	+++	+++	++	+++
CLN6 -3	±	±	+	+
CLN7	++	+	++	++

Table 3.
Immunofluorescence (IF) and western blotting (WB) analyses of LC3 expression, both at early and late stages of cultures. CLN1 -3, CLN3 -2 and CLN6 -2 show high level of this autophagic markers at both stages of culture. In general, the signal intensity of immunofluorescence assay resembles the intensity after immunoblotting analysis. ('-': no signal; '±': poor signal; '+': weak signal; '++' intense and '+++' highly intense signal; 'nd': not done)

THE MITOCHONDRIAL COMPARTMENT

Relationship between lysosomal compartment and mitochondria network in NCL

We hypothesized that the expansion of lysosomal structures in the cytoplasm of NCL fibroblasts could affect the distribution and functioning of the mitochondrial reticulum. The mitochondrial fluorescent probe Mitotracker was employed in association with Lysotracker in order to investigate the spatial relationship between mitochondrial and lysosomal compartments and to identify changes of mitochondria distribution due to abnormal lysosomal storage. The investigation of mitochondrial compartment was made principally at late stages of culture because previous date suggested that at 15th passage the engulfment by lysosomal structures was more severe.

Mitotracker staining showed that in normal fibroblasts mitochondria are organized in a tubular network. This network is mainly distributed around nucleus, forming a tubular and regular reticulum. As concerned NCL fibroblasts, cells with intense Lysotracker staining and lysosomes accumulation showed a distortion of mitochondrial network, mainly in perinuclear regions where the lysosome storage was more severe (figure 8).

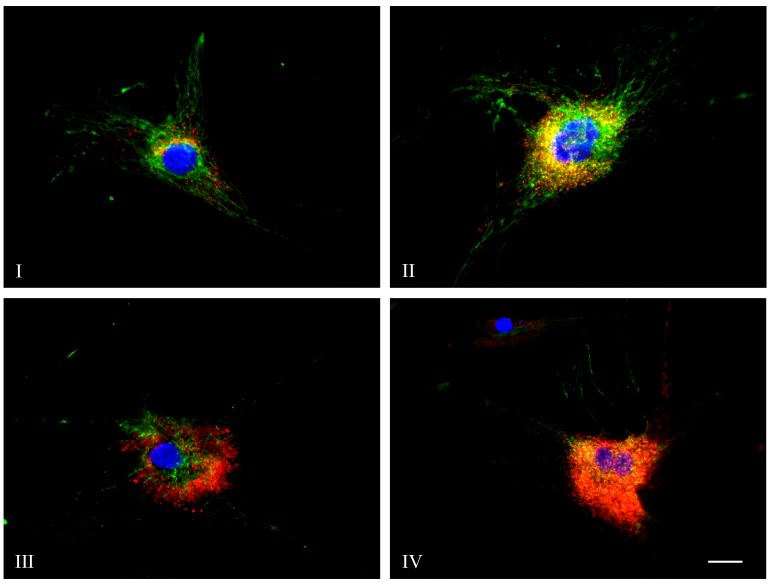

Figure 8.
Relationship between mitochondrial and lysosomal compartments at late stage of culture. Cell were exposed at the same time with Mitotracker (green) and Lysotracker (red) and counterstained by Hoechst (blue). I: the distribution of the mitochondrial reticulum through the cell body and processes; note punctuated Lysotracker staining in the perinuclear region. II: increased evidence of Lysotracker staining in the perinuclear region; a colocalized pattern is shown (yellow). III: the cytoplasm of a round cell is filled with red fluorescence; scanty Mitotracker staining can be detected in the peripheral processes. IV: even more intense lysosomal staining and stripes and filamentous pattern of mitochondrial staining at the cell periphery. (I control; II CLN1 -1; III CLN3 -2; IV CLN7). Scale bar equal to 20 µm.

In addition, we tried to quantify this morphological alteration, identifying those cells that showed a fragmented or altered distribution of mitochondria after Mitotracker staining (figure 9). We found that the percentage of cells with altered mitochondrial network after 15 passages was increased in NCL cultures as compared to control. CLN1 exhibited higher percentage as compared to control (66% for CLN1 -1 and 35% for CLN1-2 versus 10% for control cells). Moreover, also CLN1 -3, CLN5, CLN6 -1 and CLN6 -3 showed similar percentage of cells with distorted reticulum, that is higher than control ones.

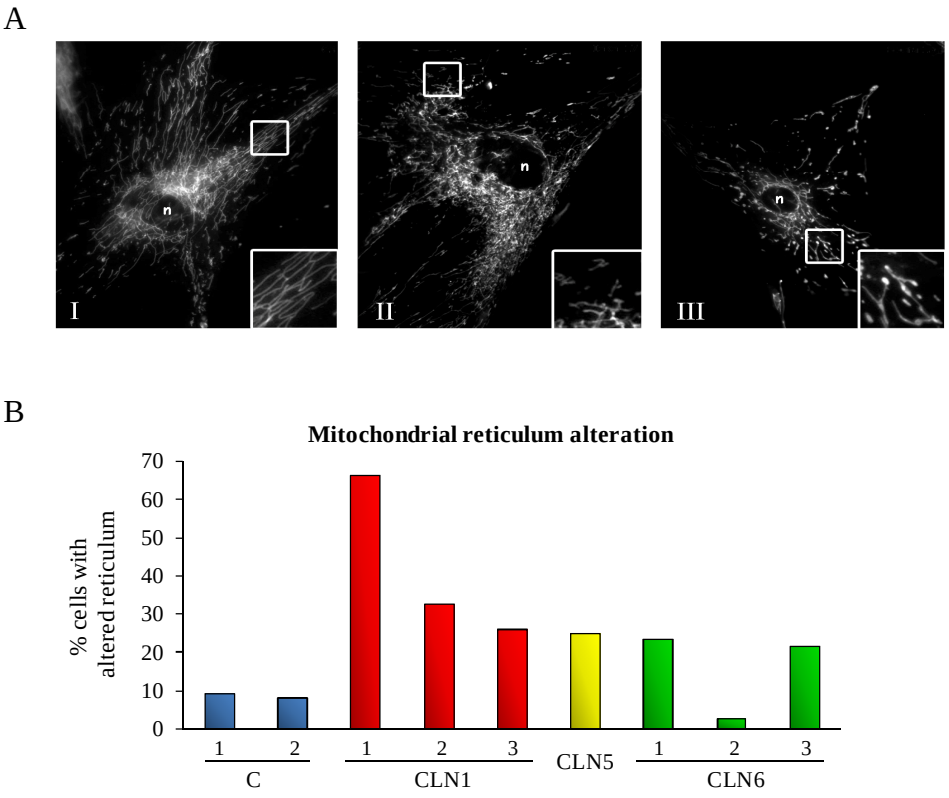

Figure 9.

A. Mitotracker staining of the mitochondrial compartment at late stages of culture. Mitochondrial reticulum appears distorted and fragmented in NCL fibroblasts, as depicted in insets (I control; II CLN1 -1; III CLN6 -1).

B. Semiquantitative analysis of mitochondrial reticulum at 15th passage. NCL lines show high percentage of cells with distorted reticulum as compared to controls, except for CLN6 -2.

Mitochondrial density and lysosomal accumulation

Following the fluorescent study of mitochondrial compartment, we performed an ultrastructural analysis in order to confirm the alteration of spatial mitochondria distribution within the NCL cytoplasm in relation with lysosomal structures. The EM analysis of fibroblast cultures confirmed that mitochondria distribution was strictly connected with the distribution of lysosomal structures. As described above, NCL fibroblasts, at 15th passage of culture, showed a remarkable amount of empty vacuoles and

lysosomal bodies, mostly located by the perinuclear region. Only a few mitochondria remained in the perinuclear area, whereas several of them could be detected at the cell periphery, as depicted for a CLN1 -2 fibroblast (figure 10A). To confirm that in NCL cell the lysosomal compartment might affect the distribution of mitochondria, we performed a semiquantitative analysis of mitochondria density. As shown in figure 10B, the number of mitochondria in perinuclear area was significant lower in 3 CLN1 and 3 CLN6 lines as compared to controls at the 16th passage in culture. In addition, we performed an immunoblotting analysis on cellular lysates from NCL and control fibroblasts in order to evaluate the ratio between the mitochondrial porin VDAC (the most abundant protein of mitochondrial outer membrane, which is considered as a quantitative marker of the cellular mitochondrial population; Rostovtseva and Bezrukov, 2008) and α-tubulin. Since the early

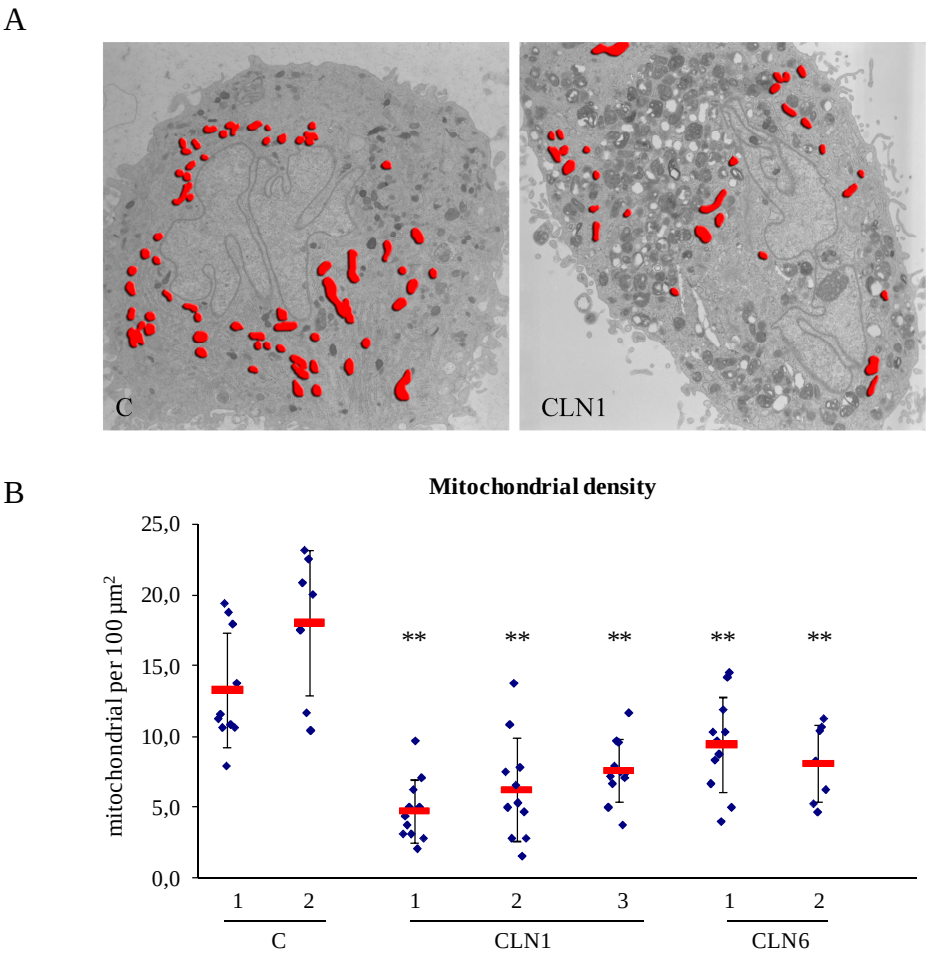

Figure 10.

A. Distribution of mitochondria, represented as red dot, in control (C1) and CLN1 -1 lines (16th passage). Few mitochondria are detected in the perinuclear area in CLN1 cell as compared to controls. Photos were acquired at 3000X magnitude.

B. Electron microscopy analysis of mitochondrial distribution in control and NCL fibroblasts in the perinuclear area (16th passage). The density of mitochondria per cell surface (100 µm^2) is lower in different NCL lines, especially in CLN1 lines (** p< 0.001).

passages, this ratio was significant lower in NCL fibroblasts as compared to controls, particularly the CLN1 lines and the CLN7 line, suggesting that the mitochondrial density is really defective since early steps of culture (figure 11). A similar trend was evident also by using another mitochondrial protein, subunit IV of cytochrome c oxidase (COX IV). However, at late passage the difference in VDAC/tub ratio is less significant than at early passages due to the increased variability of control lines.

A

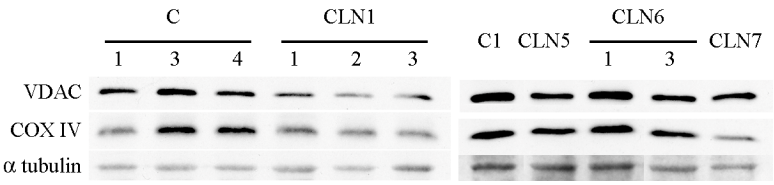

B

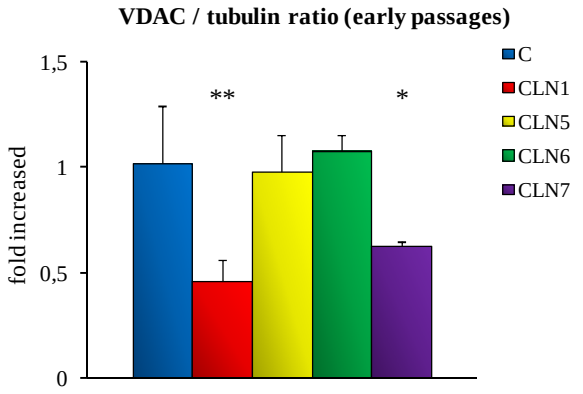

Figure 11.

A. Western blotting analysis of two mitochondrial markers, VDAC and COX IV, on control and NCL lines (early passages).

B. Quantitative analysis of VDAC/α tubulin ratio. CLN1 and CLN7 exhibit significant reduction at early passages as compared to control, whereas no difference is found for CLN5 and CLN6 lines. At late passages, differences between cases and control are less significant. Values are reported as 'fold increase' as compared to a control lysate. Histograms represent means ± deviation standard of at least two independent experiments on control and NCL lines (C: C1, C2, C3 and C4; CLN1: CLN-1, CLN1 -2 and CLN1 -3; CLN6: CLN6 -1, CLN6 -2 and CLN6 -3). Only one CLN5 and CLN7 lines were analyzed (* $p<0.05$; ** $p< 0.01$).

JC1 staining and the distribution of polarized mitochondria in NCL fibroblasts

In order to see if the modification of mitochondrial reticulum was related to a functional alteration of mitochondria in NCL fibroblasts, we investigated the mitochondrial membrane polarization state and the distribution of polarized mitochondria using JC1. By using this fluorescent probe, mitochondria with normal membrane polarization show yellow/red fluorescence, while damaged mitochondria with low $\Delta\psi m$ display green

fluorescence. NCL fibroblasts exhibited a different distribution of polarized mitochondria as compared to control fibroblasts. In the early stage of culture, several NCL cells appeared swollen and the polarized mitochondria were shifted to the cell periphery, leaving a green-staining perinuclear zone. At late stages, the number of swollen engulfed cells increased and the shift of polarized mitochondria become more evident. Only few polarized mitochondria remained in perinuclear region (figure 12). In addition, the pattern of polarized mitochondria was also different among control and NCL fibroblasts. In fact, in control cells it was possible to identify a tubular shape of red-staining polarized mitochondria, whereas in NCL fibroblasts polarized mitochondria appeared shorter and dotted.

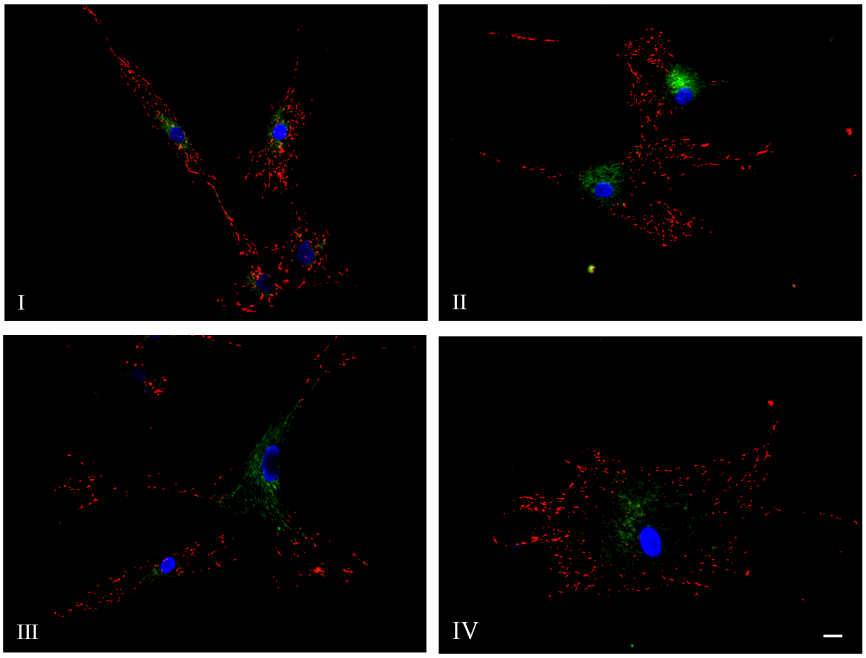

Figure 12 .
Distribution of polarized mitochondria (red) in control and NCL fibroblasts at late passages. JC1 staining shows that polarized mitochondria are delocalized to cell periphery in NCL fibroblasts (I control; II CLN1 -1; III CLN3 -1; IV CLN7). Few mitochondria remain in the perinuclear region, where the engulfment of lysosomal material is more severe. Nuclei were counterstained with Hoechst (blue). Scale bar equal to 20 µm.

Respiratory chain activity in NCL fibroblasts

In order to correlate the morphological changes with a possible functional impairment of mitochondria, we investigated the respiratory chain activity in different NCL lines at late stage of cultures. As regard the activity of complex II-III, the biochemical analysis revealed a significant reduction in CLN1 and CLN5 cell lines, whereas only CLN5 cell line had a decreased activity in the complex IV (table 4). No differences of complex I-III activity was detected among case and control fibroblasts.

	C	CLN1	CLN5	CLN6
Complex I-III	54.23 ± 4.9	63.36 ± 17.18	39.07 ± 21.28	39.75 ± 27.02
Complex II-III	0.43 ± 0.14	0.22 ± 0.02 *	0.21 ± 0.11 *	0.23 ± 0.17
Complex IV	2.45 ± 0.73	1.56 ± 0.54	0.62 ± 0.15 *	1.27 ± 0.51

Table 4.
Biochemical analysis of respiratory chain in control and NCL fibroblasts at late passages. Complex II-III activity was reduced in CLN1 and CLN5 lines, whereas complex IV was affected only in CLN5 line (* $p < 0.05$). No meaningful difference in complex I-III was found. Values are corrected for citrate synthase activity and reported as means ± standard deviation of at least two experiments on different controls and NCL lines (C: C1, C2, C3 and C4; CLN1: CLN1-, CLN1-2, CLN1-3; CLN6: CLN6-1, CLN6-2; only one CLN5 line was used).

Mitochondrial related apoptotic pathway under basal conditions and after STS exposure in NCL fibroblasts

In addition to the study of respiratory chain activity, we tested whether the mitochondrial impairment in NCL fibroblasts might activate the mitochondrial-dependent apoptotic pathway, and therefore lead to cell death *via* apoptosis. Specifically, we investigated two main late steps of the caspase dependent apoptosis, cleavage of caspase-3 and nuclear fragmentation. In basal conditions, no fragmented nuclei were detected following both DAPI nuclear staining and ultrastructural analysis in both control and NCL fibroblasts. To test differences in vulnerability to cell death among control and NCL cells, we treated cultures with Staurosporine, an inhibitor of protein kinase C (PKC), able to trigger both caspase dependent and independent apoptotic pathway and to depolarize the mitochondrial membrane potential, which eventually leads to apoptotic cell death (Johansson et al 2003; Salvioli et al 2000). Following incubation with 500 nM STS for 16 hours, fibroblasts changed their morphology, became smaller and a significant number of fragmented nuclei and cleaved caspase-3 could be detected after immunofluorescence assay and western blotting analysis (figure 13A). The immunofluorescence quantitative analysis after exposure to STS revealed a different vulnerability among the different NCL forms at early passages (figure 13B and 13C). In particular, two CLN1 cell lines (CLN1 -1 and -2) showed an high percentages of cleaved caspase-3 positive cells as compared to controls (21 and 27.5 % against 8.1%; $p < 0.001$). On the other side, cell lines belonging to 'secondary' lysosomal NCL forms (CLN5, CLN6 -2, CLN6 -3 and CLN7) showed similar level of apoptotic positive cells as compared to control. At late passages, the percentage of

fragmented nuclei and caspase-3 positive cells decreased also in the two CLN1 and no statistical significance between NCL and control lines was found (data not shown).

Preliminary investigation on the cellular density reduction associated with the activation of caspase-3 induced by STS did not provide evidence of meaningful decreased cell density among CLN1 and control cell lines. Furthermore, similar findings were obtained from the same experimental approach to the other CLN forms.

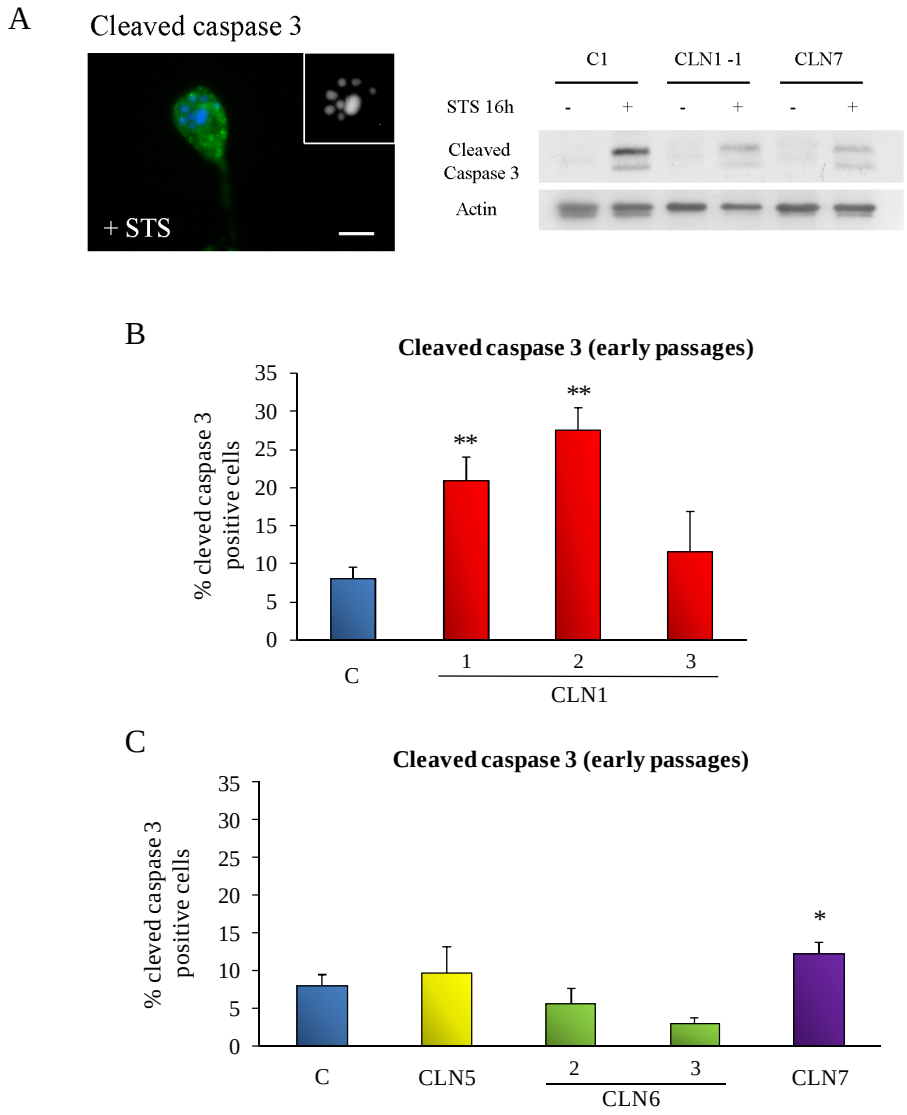

Figure 13 .
Apoptotic cell death investigation in NCL fibroblasts.
A. After 16 hours of exposure to 500 nM STS, cleaved caspase-3 positive cell with fragmented nucleus (inset) could be detected in CLN1 -2 cell line. The presence of cleaved caspase-3 was confirmed by western blotting analysis in control and NCL lines (early passages).
B and C. Percentage of cleaved caspase-3 positive cells after STS exposure (500 nM for 16 hours), as measured by immunofluorescence assay (early passages). A significant percentage of caspase-3 positive cells was found on CLN1 -1, CLN -2 and CLN7 cell lines (* $p < 0.05$; ** $p < 0.001$). Control values were reported as means ± deviation standard of 2 experiment in triplicate on 2 different controls, whereas means of a triplicate experiment were reported for the different NCL lines.

7. DISCUSSION

The aim of this doctorate project was to set up a pathogenetic study *in vitro*, using human NCL cell lines. In particular, we used fibroblast cultures established from patients affected with different genetically determined NCL forms, with either 'primary' (CLN1) or 'secondary' (CLN3, CLN5, CLN6 and CLN7) lysosomal involvement. These cell lines were analyzed in a 'prolonged culture paradigm' with the aim of studying the cellular behaviours that might be triggered in this stressful condition.

The main topic of this project was to investigate the evolution of the endo-lysosomal compartment during the long-lasting growth of NCL cells, and possibly shed light on the putative mechanisms which underlie the cell death mechanisms in these diseases.

As expected, the cytoplasmic distribution of lysosomal markers was associated with the ultrastructural evidence of remarkable increase of lysosomal elements (as compared to controls). Furthermore cells from all NCL forms showed steady increased of cytoplasmic empty vacuoles, most of them of lysosomal origin, whereas for other vacuolated figures the precise origin was not identified. The recognition of classical ultrastructural elements (such as the double membrane autophagosome, or the single membrane autolysosome) led us to realize the process of autophagy to be active in this *in vitro* model. The progressive decline of growth rate since the early passages, particularly evident of CLN1 and CLN7 cultures, was consistent with some energy dysfunction of the cell. And some results were in accordance with the involvement of the mitochondrial compartment, possibly due to the mechanical damage secondary to cytoplasmic engulfment by the storage.

Evolution of the endo-lysosomal system during the prolonged growth

Aging of control fibroblast cultures was associated mainly with changes in cellular morphology, loss of the typical 'spindle-like' shape and a progressive mitotic rate decline. Together with these features, Lamp2 immunofluorescence and Lysotracker staining showed an expansion of the endo-lysosomal compartment, a "physiological" feature of aging in cultured cells. The prolonged culture of NCL fibroblasts showed several similarities as compared to controls, but the features of the aging process appeared to occur earlier and to be more intense. Furthermore, different behaviours could be observed among the NCL forms, which might account for the specific effects on the cell of the mutated genes (and associated malfunctioning proteins), as well as of the specific growth features of each cell line.

The ultrastructural analysis of the endo-lysosomal compartment allowed us to identify qualitative differences in the typology of the storage material accumulating during the prolonged culture among the NCL forms. In CLN associated to mutations of genes coding for protein unrelated to the hydrolytic functions of the lysosomes (such as CLN3, CLN5, CLN6) increasing amount of lysosomal bodies was associated with the formation of large vacuoles. In CLN1, which is considered as a "primary" lysosomal disorder, the ultrastructural pattern was different, due to the early and persistent presence of smaller empty vacuoles, which matched that of dense bodies.

Furthermore, we found evidences in NCL fibroblasts of figures consistent with steps of autophagy, such as autophagosome formation, fused double membrane autophagosome with lysosomes, and lysosomal structures, either filled with electron dense material (autophagolysosome), or optically empty (empty vacuoles). And again different findings were found among the different forms, and these findings were partly confirmed by the biochemical investigations.

Three CLN1 lines shared a common behaviour as regards the increasing amount of empty vacuoles from early to late passages. Moreover, LC3 II was expressed in similar way in CLN1-2 and CLN1-3 and in a weaker manner in CLN1-1, both after immunofluorescence and western blot analysis. These findings, together with the Lamp2 and Lysotracker increased signal, suggested that the autophagic process may be activated in similar manner in the CLN1 lines, regardless the kind of gene mutations. The increased amount of empty vacuoles at late passages and the relative lower increasing in lysosomal bodies accumulation aroused the question of the meaning of autophagy in this condition. Moreover, it is important to keep in mind that there are no evidence of autophagy in CLN1 biopsies *in vivo*. Thus the activation of the autophagic response in our *in vitro* model probably represents a transient adaptive behaviour of cells to cope with the storage of undigested lysosomal material.

On the other hand, CLN3, CLN5 and CLN6 exhibited different behaviours as compared to CLN1 and controls; indeed, it was possible to differentiate two main patterns. CLN3-2, CLN6-2 and CLN5 showed evidences of an intense autophagic response, both at early and late steps of this process. In particular, autophagosomes (as well as empty vacuoles and autophagolysosomes) were detected in the cytoplasm and this finding was supported by high expression of LC3 II after both immunofluorescence and western blot assays. Moreover, these cell lines shared a common ultrastructural pattern, featuring decreased vacuolization and increased lysosomal bodies storage from early to late passages of

cultures. Conversely, CLN6-1 and CLN6-3 were marked by lower level of LC3 II expression at western blot analysis and an increasing vacuolization from early to late passages, even if autophagosomes were detected on CLN6 -3 cells at late passages. In CLN3-1 vacuolization and dense bodies formation was never associated with evidence of LC3 I to LC3 II conversion.

Taking together, these findings suggested that the autophagic process was activated in our *in vitro* model, unrelated to either specific NCL form or severity of mutation. At early passages, this phenomenon was expressed with a intensity gradient among the different NCL cell lines, and it was particularly evident on CLN3 -2 and CLN6 -2 (figure 14).

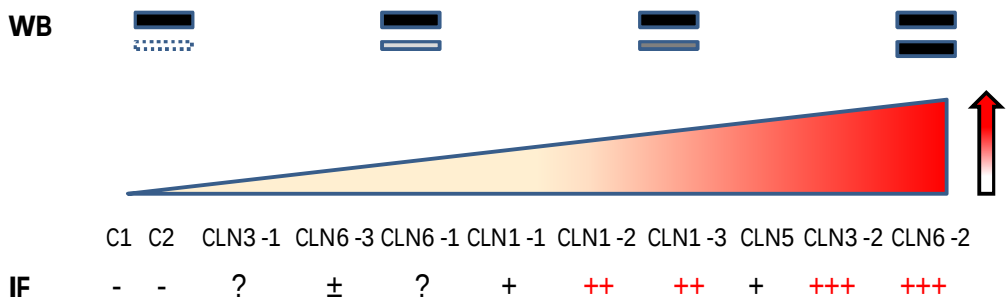

Figure 14.
Intensity gradient of LC3 expression in different NCL lines, represented for western blotting (WB, upper part) and immunofluorescence analyses (IF, lower part) at early passages. As regard IF, a score related to the amount of LC3 vesicles was given ('-' and '±': no or few LC3 positive vesicles; '+' and '++': several and many LC3 positive vesicles; '+++' high amount of LC3 positive vesicles; '?': not tested). This graph derived from figure 5, figure 7 and table 3.

Moreover, in the same cell lines, it was a long lasting process detectable even at late observations both ultrastructurally and biochemically. Vacuolization occurred early in those lines of NCL which are known to have vacuolated cells *in vivo* (such as CLN3 and CLN6), whereas its onset was later in CLN1 (which are not associated with vacuole formation *in vivo*). Nevertheless, despite a wide vacuolization of the cytoplasm in many NCL cell, we could not find evidence of autophagic cell death.

A possible interpretation of these events is far to be near. One might argue that in CLN3, CLN6, CLN5 (or at least in some cell lines according this experimental settings) autophagy is necessary for the process of lysosomal storage (and possible degradation) of the products which accumulate due to the genetic defect. As to the question whether the persistence of autophagy will provide advantages to the cells, or it will exert negative effects because it keeps on going out of control (even to possible cell death) no answer is possible right now. In fact, autophagy has been recently related to different human pathologies, including neurodegenerative disorders (Levine and Kroemer, 2008). Moreover, autophagic

impairment has been linked to LSD, on the assumption that a lysosomal defect may interfere with the normal autophagy process of the cell. Thus, evidences of autophagic impairment, such as increased LC3 II level and autophagosomes accumulation, have been described on MSD, MPS-IIIa and G_{M1} mouse brain samples (Settembre et al, 2008; Takamura et al, 2008). With regard to NCL, CLN3 was considered as the main NCL form in which autophagy is activated because of the detection of large vacuoles on peripheral lymphocyte and other tissues. Recently, this condition was also found on biopsies of CLN6 patients (Cannelli et al, 2009) whereas no evidence of autophagy on CLN1 has been reported *in vivo* so far. However, opposite conclusions have been drawn by studies on a murine models of CLN3. In the *CLN3Δex7/8* knock-in mouse disruption of autophagy is suggested at level of autophagic vacuolar maturation (Cao et al, 2006), whereas in such as cathepsin knock-in mice results show an active role of the autophagy process in the abnormal storage accumulation (Koike et al, 2005).

In conclusion we think that autophagy is activated in NCL cells, probably as a rescue process to cope with enhanced lysosomal storage. However, as far as those cell lines which show long lasting evidence of LC3 I → LC3 II conversion, one might argue that the switching off of autophagy is impaired, and that such condition might hamper the cell survival, whereas decline of LC3 II signal as well as vacuole formation might represent a good outcome for those cell lines, in which autophagy has been down-regulated (or switched off) and empty vacuoles represent the efficacy of the storage-degrading machinery. Which signals trigger the autophagic response and keep it on-going (or turning it down) is a matter of future investigations.

Mitochondrial involvement

Several previous studies have demonstrated that mitochondria exhibit morphological and functional alterations both in human and animal NCL fibroblast cultures. In particular, ovine CLN6 fibroblasts showed alterations of ATP synthase activity in different 'energy demand' conditions, whereas human CLN1 fibroblasts exhibited reduced ATP synthase activity as well as an impaired activity of the complexes II-III and IV of the respiratory chain (Das et al, 1999; Jolly et al, 2002). Enlarged mitochondria with abnormal cristae were also described in neurons of English setter dog (Jolly et al, 2002). Results from this study have given some structural evidences to these previous findings, and particularly it has been shown that CLN1 lines were affected in all the experimental settings. The mitochondrial reticulum appeared to be distorted and fragmented in CLN1, CLN5, CLN6

cell lines in the perinuclear region, where the accumulation of vacuoles and lysosomal bodies was more severe. Furthermore the topological involvement of the mitochondrial network was also supported by the evidences that polarized mitochondria where redistributed to the periphery as well as by a reduction in mitochondria density. Eventually, in CLN1, reduction of mitochondrial porine VDAC (on quantitative western blot analysis) was again consistent with a reduction of mitochondrial mass in the cell lysates, as it was supported by the ultrastructural semi-quantitative analysis, which also revealed the shift of mitochondria distribution from the perinuclear region to the cell periphery.

Evidences of mitochondrial fragmentation has been reported in other LSD models, such as *β-gal* $^{-/-}$ mouse astrocytes and MLIV human fibroblasts (Takamura et al, 2008; Jennings et al, 2006). The influence of lysosomal impairment on the fission and fusion processes of mitochondrial reticulum has not been clearly determined so far. However, in these models the morphological alterations in mitochondrial reticulum were related to an impaired functionality, such as in Ca^{2+} buffering capacity (Takamura et al, 2008). However, in our *in vitro* model, the morphological alterations and the reduced density of mitochondrial compartment that occur during the prolonged cultures did not seem to induce a meaningful functional impairment, as demonstrated by the slight respiratory chain involvement for CLN1 and CLN5 fibroblasts.

Which might be the implications for the neurons of such "secondary" involvement of the mitochondrial compartment? One issue might relate these findings to the known increased vulnerability of the neurological behaviour of children affected with any NCL form to energy-requiring conditions, such as the fever; likewise enhanced seizure activity observed in similar conditions might be related to decreased efficiency of inhibitory mechanisms to prevent convulsions. Furthermore distal degeneration of the long axons is observed in LSD, and that can be related to the mechanical obstacle to axoplasmic flow by the storage. If one takes into account that axonal flow dynamics are energy-dependent processes, any kind of mitochondrial dysfunction might hamper the bidirectional exchanges along the axonal length, which necessary for and depending from the good being of the cellular bioenergetic mechanisms.

A possible role of mitochondrial dysfunction has been also investigated in this thesis, namely its possible relationship with the cell death mechanisms. Several studies have already suggested a contribution of apoptosis in cell death, which occurs in human CLN1 and CLN2 (Riikonen et al, 2000, Hachiya et al, 2006). In both human and murine CLN1 caspase-mediated apoptosis was demonstrated to occur following ER stress and

mitochondrial membrane destabilization secondary to oxidative stress (Kim et al, 2006, Zhang et al, 2006, Wei et al, 2008). Conversely, overexpression of PPT1 protects neuroblastoma cell lines from induced apoptosis (Cho et al, 2000). Likewise the product of *CLN8* (whose mutations lead to a late-infantile variant form of NCL) seems to protect hippocampal neurons and human neuroblastoma cell lines from the NMDA-induced apoptosis, because both gene silencing and transfection with mutated *cln8* clones increased the percentage of apoptotic cells after the NMDA exposure (Vantaggiato et al, 2009).

We could not find any evidence of the apoptotic activation, such as cleaved caspase-3 and fragmented nuclei following immunofluorescence, western blot and EM analyses under basal condition, in any cell line. On the contrary evidence of apoptosis was obtained after inducing mitochondrial mediated cell death, by treating fibroblasts with STS, a protein kinase inhibitor which induce apoptosis by Cathepsin D translocation to the cytosol, followed by cytochrome c release and caspase activation (Johansson et al, 2003). In fact, there was a meaningful increased percentage of fragmented nuclei and caspase-3 positive cells in two CLN1 lines (figure 13), as compared to controls and the other NCL forms. This phenomenon was evident only at early passages, whereas no significant differences were obtained with aged fibroblasts. These findings are in agreement with the previous evidences that apoptosis is not a process common to all human NCL forms, but that it is limited to selected forms only, such as CLN1. Moreover, the evidence of a possible relationship among ER and oxidative stresses, mitochondrial membrane permeabilization and apoptosis may provide elements of further investigations as far as to target these phenomena with specific drugs (e.g. anti-oxidants), in order to slow down and ameliorate the disease progression, in CLN1 at least.

Conclusions and perspectives

In conclusion, the culture model employed in this study provided several information about the pathogenic mechanisms that could be involved in NCL, at least *in vitro*. Indeed, the expression of LC3 II, the detection of autophagosomes and single membrane vacuoles, both empty and with indigested material, in the cytoplasm of most of NCL cell lines demonstrated an involvement of the autophagic pathway. The presence of empty vacuoles is not *per se* a clue of autophagic response under way but it suggests that this process might be unable to evolve in a physiological manner. These results supported the idea that autophagy may be involved in the pathogenesis of NCL, as already demonstrated in *cln3* and cathepsin deficient mice (Koike et al, 2005; Cao et al, 2006). However, our findings

suggested that in this *in vitro* model activation of autophagy might be considered as an adaptive mechanism by which cells try to cope with the enhanced lysosomal activity rather than a direct cell death mechanism. Certainly, the role of autophagy in NCL deserves a more detailed investigation, in order to better characterize, for instance, the dynamics of this process in NCL, such as the alteration of the 'autophagic flux' in basal conditions and after modulation by chemical inducers and/or blocker (Mizushima et al, 2010). Moreover, the major goal will be to find out which signals regulate the activated autophagy, either as an effective rescue mechanism or as a condition which collaborates with storage engulfment of the cells. Thus, we can hypothesize that the study of the autophagic involvement in NCL could have a direct impact on the planning of hypothetical treatments of this disorders, that are not available so far. For instance, one might argue that if the NCL forms with prolonged survival showed a 'better' autophagic response as compared with the most severe forms, the modulation of the autophagic pathway could have likely a direct clinical implication.

Moreover, an interesting facet emerged from the autophagic study was the formation of empty vacuoles. The nature of these structures, that were present in high amount in the cytoplasm of many NCL cell lines, seemed to be of lysosomal origin, but how and which cellular compartments they arise from remain to be clearly elucidated. Preliminary observations suggested a possible relation between expanded ER cisternae, vacuoles and autophagy and, therefore, the role of ER in NCL will be investigated in detail.

In addition, we have also demonstrated that the mitochondrial compartment may be secondarily involved in NCL. Moreover, the apoptotic study outlined a different vulnerability to STS between CLN1 and other NCL forms. Certainly, the cell death mechanism need more exhaustive studies to assess clearly distinct behaviours among the different NCL forms. It is noteworthy that fibroblasts are not so prone to undergo to apoptosis and this could be an important drawback of this *in vitro* model when compared to neuronal cell. However, the role of apoptosis in NCL has been recently revaluated. The deletion of Bax on cathepsin D mouse fails to protect the animal from neurodegeneration (Shacka et al, 2007); in addition, over-expression of Bcl-2 or knock out of p53 do not modify the lifespan of CLN2 $^{-/-}$ mouse model (Kima et al, 2009). These findings imply that the apoptotic pathway does not explain *per se* the neurodegeneration that occur in NCL and that other mechanisms could be involved in the disease progression. Moreover, murine CLN1 and CLN2 fibroblast are apparently more resistant to TNF-induced apoptosis (Tardy et al, 2009, Autefage et al, 2009). Thus, our results support the idea that in NCL other

factors than apoptosis could be involved in the pathogenesis and in cell death. We wonder if the autophagic impairment and a slight mitochondrial involvement could represent 'chronic' negative events that might enhance the vulnerability of neuronal cells to the storage-related stress, thus contributing to their fatal outcome.

Finally, we can state that the prolonged growth paradigm employed in this study was very useful to elucidate several pathological facets that occur in NCL fibroblast cultures. We are confident that this *in vitro* study could be applied to other lysosomal storage diseases, in order to elucidate behavioural similarities and/or differences between NCL and other LSD fibroblast cell lines. On the other side, we were aware of the limitation to use fibroblasts in the investigation of NCL, a group of diseases which affects the CNS primarily. However, the pathological study employed in this thesis could be translated to other experimental models, such as primary neurons cultures and neuroblastoma cell lines in order to investigate, for instance, the impact of autophagic dysfunction in neuronal cells. Moreover, also the study of vertebrate models, such as *caenorhabditis elegans* or zebrafish, could be generate new insights into the pathological changes in NCL. In particular, the use of genetically modified animal models could allow to investigate the changes which affect the CNS during the aging process, in the same as we have analyzed fibroblasts in the long-lasting growth paradigm.

8. REFERENCES

Ahtiainen L, Luiro K, Kauppi M, Tyynelä J, Kopra O, Jalanko A. Palmitoyl protein thioesterase 1 (PPT1) deficiency causes endocytic defects connected to abnormal saposin processing. *Exp Cell Res.* 2006; 312: 1540-1553.

Ahtiainen L, van Diggelen OP, Jalanko A, Kopra O. Palmitoyl protein thioesterase 1 is targeted to the axons in neurons. *J Comp Neurol.* 2003; 455: 368-377.

Aiello C, Terracciano A, Simonati A, Discepoli G, Cannelli N, Claps D, Crow YJ, Bianchi M, Kitzmuller C, Longo D, Tavoni A, Franzoni E, Tessa A, Veneselli E, Boldrini R, Filocamo M, Williams RE, Bertini ES, Biancheri R, Carrozzo R, Mole SE, Santorelli FM. Mutations in MFSD8/CLN7 are a frequent cause of variant-late infantile neuronal ceroid lipofuscinosis. *Hum Mutat*. 2009; 30: E530-540.

Autefage H, Albinet V, Garcia V, Berges H, Nicolau M-L, Therville N, Altie M-F, Caillaud C, Levade T, Andrieu-Abadie N. Lysosomal serine protease CLN2 regulates tumor necrosis factor-mediated apoptosis in a Bid-dependent manner. *J Biol Chem.* 2009; 17: 11507-11516.

Ballabio A, Gieselmann V. Lysosomal disorders: from storage to cellular damage. *Biochim Biophys Acta*. 2009; 1793: 684-896.

Bellizzi III JJ, Widom J, Kemp C, Lu JY, Das AK, Hofmann SL, Clardy J. The crystal structure of palmitoyl protein thioesterase 1 and the molecular basis of infantile neuronal ceroid lipofuscinosis. *Proc Natl Acad Sci U. S. A.* 2000; 97: 4573-4578.

Benes P, Vetvicka V, Fusek M. Cathepsin D - many functions of one aspartic protease. *Crit Rev Oncol Hematol.* 2008; 68: 12-28.

Bessa C, Teixeira CA, Mangas M, Dias A, Sá Miranda MC, Guimãraes A, Ferreira JC, Canas N, Cabral P, Ribeiro MG. Two novel CLN5 mutations in a Portuguese patient with vLINCL: insights into molecular mechanisms of CLN5 deficiency. *Mol Gen Metab.* 2006; 89: 245-253.

Camp LA, Hofmann SL. Purification and properties of a palmitoyl-protein thioesterase that cleaves palmitate from H-Ras. *J Biol Chem*. 1993; 268: 22566-22574.

Cannelli N, Cassandrini D, Bestini E, Striano P, Fusco L, Caggero R, Specchio N, Biancheri R, Vigevano R, Bruno C, Simonati A, Zara F, Santorelli FM. Novel mutations in CLN8 in Italian variant late infantile neuronal ceroid lipofuscinosis: another genetic hit in the Mediterranian. *Neurogenetics*. 2006; 7: 111-117.

Cannelli N, Garavaglia B, Simonati A, Aiello C, Barzaghi C, Pezzini F, Cilio MR, Biancheri R, Morbin M, Dalla Bernardina B, Granata T, Tessa A, Invernizzi F, Pessagno A, Boldrini R, Zibordi F, Grazian L, Claps D, Carrozzo R, Mole SE, Nardocci N, Santorelli FM. Variant Late Infantile Ceroid Lipofuscinoses associated with novel mutations in *CLN6. Biochem Biophys Res Commun*. 2009; 379: 892-897.

Cannelli N, Nardocci N, Cassandrini D, Morbin M, Aiello C, Bugiani M, Criscuolo L, Zara F, Striano P, Granata T, Bestini E, Simonati A, Santorelli FM. Revelation of a novel CLN5 mutation in early juvenile neuronal ceroid lipofuscinosis. *Neuropediatrics.* 2007; 38: 46-49.

Cao Y, Espinola JA, Fossale E, Massey AC, Cuervo AM, MacDonald ME, Cotman SL. Autophagy is disrupted in a knock-in mouse model of juvenile neuronal ceroid lipofuscinosis. *J Biol Chem*. 2006; 281: 20483-20493.

Cho S, Dawson G. Palmitoyl protein thioesterase 1 protects against apoptosis mediated by Ras-Akt-caspase pathway in neuroblastoma cells. *J Neurochem.* 2000; 74: 1478-1488.

Cho S, Dawson PE, Dawson G. Antisense palmitoyl protein thioesterase 1 (PPT1) treatment inhibits PPT1 activity and increases cell death in LA-N-5 neuroblastoma cells. *J Neurosci Res*. 2000; 62: 234-240.

Cooper JD, Russell C, Mitchison HM. Progress towards understanding disease mechanisms in small vertebrate models of neuronal ceroid lipofuscinosis. *Biochim Biophys Acta*. 2006; 1762: 873-889.

Das AM, Jolly RD, Kohlschütter A. Anomalies of mitochondrial ATP synthase regulation in four different types of neuronal ceroid lipofuscinosis. *Mol Genet Metab.* 1999; 66: 349-355.

Dawson G, Schroeder C, Dawson PE. Palmitoyl protein thioesterase (PPT1) inhibitors can act as pharmacological chaperones in infantile Batten disease. *Biochem Biophys Res Commun* 2010; 395: 66-69.

DiMauro S, Servidei S, Zeviani M, DiRocco M, DeVivo DC, DiDonato S, Uziel G, Berry K, Hoganson G, Johnsen SD, et al. Cytochrome c oxidase deficiency in Leigh syndrome. *Ann Neurol*. 1987; 22: 498-506.

Eskelinen EL. To be or not to be? Examples of incorrect identification of autophagic compartments in conventional transmission electron microscopy of mammalian cells. *Autophagy*. 2008; 4: 257-260.

Ezaki J, Tanica I, Kanehagi N, Kominami E. A lysosomal proteinase, the late infantile neuronal ceroid lipofuscinosis gene (CLN2) product, is essential for degradation of a hydrophobic protein, the subunit c of ATP synthase. *J Neurochem.* 1999; 72: 2573-2582.

Ferri KF, Kroemer G. Organelle-specific initiation of cell death pathways. *Nat Cell Biol*. 2001; 3: E255-263.

Gachet Y, Codlin S, Hyams JS, Mole SE. btn1, the *Schizosaccharomyces pombe* homologue of the human Batten disease gene CLN3, regulates vacuole homeostasis. *J Cell Sci*. 2005; 118: 5525-5536.

Genge J, Klionsky DJ. The Atg8 and Atg12 ubiquitin-like conjugation systems in macroautophagy. *EMBO reports.* 2008; 9: 859-864.

Golabek AA, Kida E, Walus M, Wujek P, Mehta P, Wisniewski KE. Biosynthesis, glycosylation, and enzymatic processing in vivo of human tripeptidyl-peptidase I. *J Biol Chem*. 2003; 278: 7135-7145.

Golabek AA, Wujek P, Walus M, Bieler S, Soto C, Wisniewski KE, Kida E. Maturation of human tripeptidyl-peptidase I in vitro. *J Biol Chem*. 2004; 279: 31058-31067.

Goswami R, Ahmed M, Kilkus J, Han T, Dawson SA, Dawson G. Differential regulation of ceramide in lipid-rich microdomains (rafts): antagonistic role of palmitoyl:protein thioesterase and neutral sphingomyelinase 2. *J Neurosci Res.* 2005; 81: 208-217.

Guhaniyogi J, Sohar I, Das K, Stock AM, Lobel P. Crystal structure and autoactivation pathway of the precursor form of human tripeptidyl-peptidase 1, the enzyme deficient in late infantile ceroid lipofuscinosis. *J Biol Chem*. 2009; 284: 3985-3997.

Hachiya Y, Hayashi M, Uchiyama A, Tsuchiya K, Kurata K. Mechanisms of neurodegeneration in neuronal ceroid-lipofuscinoses. *Acta Neuropathol*. 2006; 111:168-177.

Haines RL, Codlin S, Mole SE. The fission yeast model for the lysosomal storage disorder Batten disease predicts disease severity caused by mutations in CLN3. *Dis Models Mech*. 2009; 2: 84-92.

Haltia M. The neuronal ceroid-lipofuscinoses: from past to present. *Biochim Biophys Acta*. 2006; 1762: 850-856.

Haskell RE, Carr CJ, Pearce DA, Bennett MJ, Davidson BL. Batten disease: evaluation of CLN3 mutations on protein localization and function. *Hum Mol Genet*. 2000; 9: 735-744.

Heine C, Koch B, Storch S, Kohlshutter A, Palmer DN, Braulke T. Defective endoplasmic reticulum-resident membrane protein CLN6 affects lysosomal degradation of endocytosed arylsulfatase A. *J Biol Chem*. 2004; 279: 22347-22352.

Heinonen O, Kyttala A, Lehmus E, Paunio T, L. Peltonen L, Jalanko A. Expression of palmitoyl protein thioesterase in neurons. *Mol Genet Metab*. 2000; 69: 123-129.

Hellsten E, Vesa J, Olkkonen VM, Jalanko A, Peltonen L. Human palmitoyl protein thioesterase: evidence for lysosomal targeting of the enzyme and disturbed cellular routing in infantile neuronal ceroid lipofuscinosis. *EMBO J*. 1996; 15: 5240-5245.

Hermansson M, Kakela R, Berghall M, Lehesjoki AE, Somerharju P, Lahtinen U. Mass spectrometric analysis reveals changes in phospholipids, neutral sphingolipid and sulfatide molecular species in progressive epilepsy with mental retardation EPMR brain: a case study. *J Neurochem.* 2005; 95: 609-617.

Holmberg V, Jalanko A, Isosomppi J, Fabritius AL, Peltonen L, Kopra O. The mouse ortholog of the neuronal ceroid lipofuscinosis CLN5 gene encodes a soluble lysosomal glycoprotein expressed in the developing brain. *Neurobiol Dis*. 2004; 16: 29-40.

Holopainen JM, Saarikoski J, Kinnunen PK, Jarvela I. Elevated lysosomal pH in neuronal ceroid lipofuscinoses (NCLs). *Eur J Biochem*. 2001; 268: 5851-5856.

Huang K, El-Husseini A. Modulation of neuronal protein trafficking and function by palmitoylation. *Curr Opin Neurobiol*. 2005; 15: 527-535.

Husseini A, Bredt DS. Protein palmitoylation: a regulator of neuronal development and function. *Nat Rev*. 2002; 3: 791-802.

Isosomppi J, Vesa J, Jalanko A, Peltonen L. Lysosomal localization of the neuronal ceroid lipofuscinosis CLN5 protein. *Hum Mol Genet*. 2002; 11: 885-891.

Jalanko A, Braulke T. Neuronal ceroid lipofuscinoses. *Biochim Biophys Acta*. 2009; 1793: 697-709.

Jalanko A, Tyynelä J, Peltonen L. From genes to systems: new global strategies for the characterization of NCL biology. *Biochim Biophys Acta*. 2006; 1762: 934-944.

Järvelä,M. Lehtovirta, R. Tikkanen, A. Kyttälä, A. Jalanko. Defective intracellular transport of CLN3 is the molecular basis of Batten disease (JNCL). *Hum Mol Genet*. 1999; 8: 1091-1098.

Jennings JJ Jr, Zhu JH, Rbaibi Y, Luo X, Chu CT, Kiselyov K. Mitochondrial aberrations in mucolipidosis Type IV. *J Biol Chem.* 2006; 281: 39041-39050.

Johanssonn AC, Steen H, Ollinger K, Roberg K. Cathepsin D mediates cytochrome c release and caspase activation in human fibroblast apoptosis induced by staurosporine. *Cell Death Differ*. 2003; 10: 1253-1259.

Jolly RD, Brown S, Das AM, Walkley SU. Mitochondrial dysfunction in the neuronal ceroid-lipofuscinoses (Batten disease). *Neurochem Int*. 2002; 40: 565-571.

Kerr JF, Wyllie AH, Currie AR. Apoptosis: a basic biological phenomenon with wide-ranging implications in tissue kinetics. *Br J Cancer*. 1972; 26: 239-257.

Kim SJ, Zhang Z, Hitomi E, Lee YC, Mukherjee AB. Endoplasmic reticulum stress-induced caspase-4 activation mediates apoptosis and neurodegeneration in INCL. *Hum Mol Genet.* 2006; 15: 1826-1834.

Kim SJ, Zhang Z, Lee YC, Mukherjee AB. Palmitoyl-protein thioesterase-1 deficiency leads to the activation of caspase-9 and contributes to rapid neurodegeneration in INCL. *Hum Mol Genet*. 2006; 15: 1580-1586.

Kima K-H, Sleata DE, Bernardd O, Lobel P. Genetic modulation of apoptotic pathways fails to alter disease course in tripeptidyl-peptidase 1 deficient mice. *Neuroscience Letters.* 2009; 45327-45330.

Kohlschütter A, Schulz A. Towards understanding the neuronal ceroid lipofuscinoses. *Brain Dev.* 2009; 31: 499-502.

Koike M, Shibata M, Waguri S, Yoshimura K, Tanida I, Kominami E, Gotow T, Peters C, von Figura K, Mizushima N, Saftig P, Uchiyama Y. Participation of autophagy in storage of lysosomes in neurons from mouse models of Neuronal Ceroid-Lipofuscinoses (Batten Disease). *Am J Pathol.* 2005; 167: 1713-1728.

Kroemer G, Galluzzi L, Vandenabeele P, Abrams J, Alnemri ES, Baehrecke EH, Blagosklonny MV, El-Deiry WS, Golstein P, Green DR, Hengartner M, Knight RA, Kumar S, Lipton SA, Malorni W, Nunez G, Peter ME, Tschopp J, Yuan J, Piacentini M, Zhivotovsky B, Melino G. Classification of cell death: recommendations of the Nomenclature Committee on Cell Death 2009. *Cell Death Differ*. 2009; 16: 3-11

Kroemer G, Jäättelä M. Lysosomes and autophagy in cell death control. *Nat Rev Cancer*. 2005; 5: 886-897.

Lebrun AH, Storch S, Ruschendorf F, Schmiedt ML, Kyttälä A, Mole SE, Kitzmüller C, Saar K, Mewasingh LD, Boda V, Kohlschutter A, Braulke T, Schulz A. Retention of lysosomal protein CLN5 in the endoplasmic reticulum causes neuronal ceroid lipofuscinosis in Asian sibships. *Hum Mutat.* 2009; 30: E651-61

Lehtovirta M, Kyttälä A, Eskelinen EL, Hess M, Heinonen O, Jalanko A. Palmitoyl protein thioesterase (PPT) localizes into synaptosomes and synaptic vesicles in neurons: implications for infantile neuronal ceroid lipofuscinosis (INCL). *Hum Mol Genet.* 2001; 10: 69-75.

Levine B, Kroemer G. Autophagy in the pathogenesis of disease. *Cell.* 2008; 132: 27-42.

Lonka L, Kyttala A, Ranta S, Jalanko A, Lehesjoki AE. The neuronal ceroid lipofuscinosis CLN8 membrane protein is a resident of the endoplasmic reticulum. *Hum Mol Genet*. 2000; 9: 1691-1697.

Lonka L, Salonen T, Siintola E, Kopra O, Lehesjoki AE, Jalanko A. Localization of wild-type and mutant neuronal ceroid lipofuscinosis CLN8 proteins in non neuronal and neuronal cells. *J Neurosci Res.* 2004; 76: 862-871.

Lubke T, Lobel P, Sleat DE. Proteomics of the lysosome. *Biochim Biophys Acta*. 2009; 1793: 625-35.

Lyly A, von Schantz C, Heine C, Schmiedt ML, Sipilä T, Jalanko A, Kyttälä A. Novel interactions of CLN5 support molecular networking between Neuronal Ceroid Lipofuscinosis proteins. *BMC Cell Biol*. 2009; 10: 83.

Lyly A, von Schantz C, Saloanen T, Kopra O, Saarela J, Jauhiainen M, Kyttälä A, Jalanko A. Glycosylation, transport, and complex formation of palmitoyl protein thioesterase 1 (PPT1) – distinct characteristics in neurons. *BMC Cell Biol.* 2007; 8: 22.

Maiuri MC, Zalckvar E, Kimchi A, Kroemer G. Self-eating and self-killing: crosstalk between autophagy and apoptosis. *Nature Rev Mol Cell Biol.* 2007; 8: 743-752.

Mizushima N, Levine B, Cuervo AM, Klionsky DJ. Autophagy fights disease through cellular self-digestion. *Nature*. 2008; 451: 1069-1075.

Mizushima N, Yoshimori T. How to interpret LC3 immunoblotting. *Autophagy*. 2007; 3: 542-545.

Mizushima N, Yoshimori T, Levine B. Methods in mammalian autophagy research. *Cell*. 2010; 140: 313-326.

Mole SE, Williams RE, Goebel HH. Correlations between genotype, ultrastructural morphology and clinical phenotype in the neuronal ceroid lipofuscinoses. *Neurogenetics*. 2005; 6: 107-126.

Pal A, Kraetzner R, Gruene T, Grapp M, Schreiber K, Grønborg M, Urlaub H, Becker S, Asif AR, Gärtner J, Sheldrick GM, Steinfeld R. Structure of tripeptidyl-peptidase I provides insight into the molecular basis of late infantile neuronal ceroid lipofuscinosis. *J Biol Chem*. 2009; 284: 3976-3984.

Palmer DN, Fearnley IM, Walker JE, Hall NA, Lake BD, Wolfe LS, Haltia M, Martinus RD, Jolly RD. Mitochondrial ATP synthase subunit c storage in the ceroid-lipofuscinoses (Batten disease). *Am J Med Genet.* 1992; 42: 561-567.

Prescott GR, Gorleku OA, Greaves J, Chamberlain LH. Palmitoylation of the synaptic vesicle fusion machinery. *J Neurochem*. 2009; 110: 1135-1149.

Ranta S, Topcu M, Tegelberg S, Tan H, Üstübütün, A Saatci I, Dufke A, Enders H, Pohl K, Alembik Y, Mitchell WA, Mole SE, Lehesjoki AE. Variant late infantile neuronal ceroid lipofuscinosis in a subset of Turkish patients is allelic to northern epilepsy. *Hum Mutat*. 2004; 23: 300-305.

Ranta S, Zhang Y, Ross B. The neuronal ceroid-lipofuscinoses in human EPMR and mnd mutant mice are associated with mutations in CLN8. *Nat Genet*. 1999; 23: 233-236.

Riebeling C, Allegood JC, Wang E, Merrill Jr AH, Futerman AH. Two mammalian longevity assurance gene (LAG1) family members, trh1 and trh4, regulate dihydroceramide synthesis using different fatty acyl-CoA donors. *J Biol Chem*. 2003; 278: 43452-43459.

Riikonen R, Vanhanen S-L, Tyynela J, Santavuori P, Turpeinen U. CSF insulin-like growth factor-1 in infantile ceroid lipofuscinosis. Neurology 2000; 54: 1828-1832.

Rostovtseva TK, Bezrukov SM. VDAC regulation: role of cytosolic proteins and mitochondrial lipids. *J Bioenerg Biomembr*. 2008;40: 163-170.

Rusyn E, Mousallem T, Persaud-Sawin DA, Miller S, Boustany RM. CLN3p impacts galactosylceramide transport, raft morphology, and lipid content. *Pediatr Res*. 2008; 63: 625-631.

Saftig P, Klumperman J. Lysosome biogenesis and lysosomal membrane proteins: trafficking meets function. *Nat Rev Mol Cell Biol*. 2009; 10: 623-635.

Salvioli S, Dobrucki J, Moretti L, Troiano L, Fernandez MG, Pinti M, Pedrazzi J, Franceschi C, Cossarizza A. Mitochondrial heterogeneity during staurosporine-induced apoptosis in HL60 cells: analysis at the single cell and single organelle level. *Cytometry*. 2000; 40: 189-197.

Savukoski M, Klockars T, Holmberg V, Santavuori P, Lander ES, Peltonen L. CLN5, a novel gene encoding a putative transmembrane protein mutated in Finnish variant late infantile neuronal ceroid lipofuscinosis. *Nat Genet.* 1998; 19: 286-288.

Schmiedt ML, Bessa C, Heine C, Gil Ribeiro M, Jalanko A, Kyttälä A. The neuronal ceroid lipofuscinosis protein CLN5: New insights into cellular maturation, transport and consequences of mutations. *Hum Mutat.* 2010; 31: 356-365.

Schultz A, Dhar S, Rylova S, Dbaibo G, Alroy J, Hagel C, Artacho I, Kohlschütter A, Lin S, Boustany RM. Impaired cell adhesion and apoptosis in a novel CLN9 Batten disease variant. *Ann Neurol*. 2004; 56: 342-350.

Schultz A, Mousallem T, Venkataramani M, Persaud-Sawin DA, Zucker A, Luberto C, Bielawska A, Bielawski J, Holthuis JC, Jazwinski SM, Kozhaya L, Dbaibo GS, Boustany RM. The CLN9 protein, a regulator of dihydroceramide synthase. *J Biol Chem.* 2006; 281: 2784-2794.

Settembre C, Fraldi A, Jahreiss L, Spampanato C, Venturi C, Medina D, de Pablo R, Tacchetti C, Rubinsztein DC, Ballabio A. A block of autophagy in lysosomal storage disorders. *Hum Mol Genet.* 2008; 17: 119-129.

Shacka JJ and KA Roth. Cathepsin D deficiency and NCL/Batten disease: there's more to death than apoptosis. *Autophagy.* 2007; 3: 474-476.

Shacka JJ, Klocke BJ, Young C, Shibata M, Olney JW, Uchiyama Y, Saftig P, Roth KA. Cathepsin D deficiency induces persistent neurodegeneration in the absence of Bax-dependent apoptosis. *J Neurosci*. 2007; 27: 2081-2090.

Siintola E, Partanen S, Stromme P, Haapanen A, Haltia M, Maehlen J, Lehesjoki AE, Tyynela J. Cathepsin D deficiency underlies congenital human neuronal ceroid-lipofuscinosis. *Brain*. 2006; 129: 1438-1445.

Siintola E, Topcu M, Aula N, Lohi H, Minassian BA, Paterson AD, Liu XQ, Wilson C, Lahtinen U, Anttonen AK, Lehesjoki AE. The novel neuronal ceroid lipofuscinosis gene MFSD8 encodes a putative lysosomal transporter. *Am J Hum Genet.* 2007; 81: 136-146.

Simonati A, Cannelli N, Pezzini F, Aiello C, Bianchi M, Tessa A, Santorelli FM. Neuronal ceroid lipofuscinoses: many players and more to come. *Future Neurology.* 2009; 4: 601-616.

Sleat DE, Donnelly RJ, Lackland H, Liu CG, Sohar I, Pullarkat RK, Lobel P. Association of mutations in a lysosomal protein with classical late-infantile neuronal ceroid lipofuscinosis. *Science.* 1997; 277: 1802-1805.

Sleat DE, Zheng H, Qian M, Lobel P. Identification of sites of mannose 6-phosphorylation on lysosomal proteins. *Mol Cell Proteomics.* 2006; 5: 686-701.

Sleat DE, Jadot M, Lobel P. Lysosomal proteomics and disease. *Proteomics-Clinical Applications.* 2007; 1: 1134-1146

Steinfeld R, Reinhardt K, Schreiber K, Hillebrand M, Kraetzner R, Bruck W, Saftig P, Gartner J. Cathepsin D deficiency is associated with a human neurodegenerative disorder. *Am J Hum Genet.* 2006; 78: 988-998.

Takamura A, Higaki K, Kajimaki K, Otsuka S, Ninomiya H, Matsuda J, Ohno K, Suzuki Y, Nanba E. Enhanced autophagy and mitochondrial aberrations in murine G_{M1}-gangliosidosis. *Biochem Biophys Res Commun.* 2008; 367: 616-622.

Tardy C, Sabourdy F, Garcia V, Jalanko A, Therville N, Levade T, Andrieu-Abadie N. Palmitoyl protein thioesterase 1 modulates tumor necrosis factor α-induced apoptosis. *Biochim Biophys Acta*. 2009; 1793: 1250-1258.

Tasdemir E, Galluzzi L, Maiuri MC, Criollo A, Vitale I, Hangen E, Modjtahedi N, Kroemer G. Methods for assessing autophagy and autophagic cell death. *Methods Mol Biol*. 2008; 445: 29-76.

The International Batten Disease Consortium. Isolation of a novel gene underlying Batten disease, CLN3. *Cell*. 1995; 82: 949-957.

van Diggelen OP, Thobois S, Tilikete C, Zabot MT, Keulemans JL, van Bunderen PA, Taschner PE, Losekoot M, Voznyi YV. Adult neuronal ceroid lipofuscinosis with palmitoyl protein thioesterase deficiency: first adult-onset patients of a childhood disease. *Ann Neurol*. 2001; 50: 269-272.

Vantaggiato C, Redaelli F, Falcone S, Perrotta C, Tonelli A, Bondioni S, Morbin M, Riva D, Saletti V, Bonaglia MC, Giorda R, Bresolin N, Clementi E, Bassi MT. A novel CLN8 mutation in late-infantile-onset neuronal ceroid lipofuscinosis (LINCL) reveals aspects of CLN8 neurobiological function. *Hum Mutat*. 2009; 30: 1104-1116.

Vellodi A. Lysosomal storage disorders. *Br J Haematol*. 2005; 128: 413-431.

Vergarajauregui S, Connelly PS, Daniels MP, Puertollano R. Autophagic dysfunction in mucolipidosis type IV patients. *Hum Mol Genet*. 2008; 17: 2723-2737.

Verkruyse LA, Hofmann SL. Lysosomal targeting of palmitoyl-protein thioesterase. *J Biol Chem*. 1996; 271: 15831-15836.

Vesa J, Chin MH, Oelgeschläger K, Isosomppi J, DellAngelica EC, Jalanko A, Peltonen L. Neuronal ceroid lipofuscinoses are connected at molecular level: interaction of CLN5 protein with CLN2 and CLN3. *Mol Biol Cell*. 2002; 13: 2410-2420.

Vesa J, Hellsten E, Verkruyse LA, Camp LA, Rapola J, Santavuori P, Hofmann SL, Peltonen L. Mutations in the palmitoyl protein thioesterase gene causing infantile neuronal ceroid lipofuscinosis. *Nature*. 1995; 376: 584-587.

Walkley SU, Vanier MT. Secondary lipid accumulation in lysosomal disease. *Biochim Biophys Acta*. 2009; 1793: 726-736.

Walkley SU. Pathogenic cascades in lysosomal disease-Why so complex? *J Inherit Metab Dis*. 2009; 32: 181-189.

Walus M, Kida E, Wisniewski KE, Golabek AA. Ser475, Glu272, Asp276, Asp327, and Asp360 are involved in catalytic activity of human tripeptidyl-peptidase I. *FEBS Lett*. 2005; 579: 1383-1388.

Wei H, Kim S-J, Zhang Z, Tsai P-C, Wisniewski KE, Mukherjee AB. ER and oxidative stresses are common mediators of apoptosis in both neurodegenerative and non-neurodegenerative lysosomal storage disorders and are alleviated by chemical chaperones. *Hum Mol Genet*. 2008; 17: 469-477.

Winslow AR, Rubinsztein DC. Autophagy in neurodegeneration and development. *Biochim Biophys Acta*. 2008; 1782: 723-729.

Winter E, Ponting CP. TRAM, LAG1 and CLN8: members of a novel family of lipid-sensing domains? *Trends Biochem Sci.* 2002; 27: 381-383.

Wujek P, Kida E, Walus M, Wisniewski KE, Golabek AA. N-glycosylation is crucial for folding, trafficking, and stability of human tripeptidyl-peptidase I. *J Biol Chem.* 2004; 279: 12827-12839.

Zaidi N, Maurer A, Nieke S, Kalbacher H. Cathepsin D: a cellular roadmap. *Biochem Biophys Res Commun.* 2008; 376: 5-9.

Zelnik N, Mahajna M, Iancu TC, Sharony R, Zeigler M. A novel mutation of the CLN8 gene: is there a Mediterranian phenotype? *Pediatr Neurol.* 2007; 36: 411-413.

Zeman W and Dyken P Neuronal ceroid-lipofuscinosis (Batten's disease). Relationship to amaurotic familial idiocy? *Pediatrics.* 1969; 44: 570-583.

Zeman W, Donahue S, Dyken P, Green J. The neuronal ceroid-lipofuscinoses (Batten-Vogt syndrome). In Leukodystrophies an Polyodystrophies, PJ Vinken and GW Bruyn eds Handbook of Clinical Neurology Chapter 10, 1970, North-Holland Publishing Co, Amsterdam, pp 588-679.

Zhang Z, Lee YC, Kim S-J, Choi M-S, Tsai PC, Xu Y, Xiao YJ, Zhang P, Heffer A, Mukherjee AB. Palmitoyl-protein thioesterase-1 deficiency mediates the activation of the unfolded protein response and neuronal apoptosis in INCL. *Hum Mol Genet.* 2006; 15: 337-346.